NRC Research Press

ARTICLE

A state-space spatial survey-based stock assessment (SSURBA) model to inform spatial variation in relative stock trends

Rajeev Kumar, Noel G. Cadigan, Nan Zheng, Divya A. Varkey, and M. Joanne Morgan

Abstract: An age-structured, spatial survey-based assessment model (SSURBA) is developed and applied to the Grand Banks stock (NAFO Divisions 3LNO) of American plaice (*Hippoglossoides platessoides*) in Newfoundland and Labrador. The state-space model is fit to annual spatial (i.e., three divisions) stock size-at-age research vessel (RV) survey indices that are assumed to be proportional to abundance. We model index catchability (q) as a logistic function of fish length, which varies with age, cohort, and the time of the survey; therefore, the model facilitates the estimation of q values that change spatially and temporally following changes in fish growth and survey gears. The SSURBA model produces division-level estimates of fishing mortality rates (F), stock productivity, and stock size relative to the logistic catchability assumption with $q = 1$ for fully selected ages. The spatial model allows us to include additional survey information compared with the space-aggregated assessment model (all of 3LNO) that is currently used to assess stock status. The model can provide estimates of relative catch, which we compare with reported catch trends to partially validate the model.

Résumé : Un modèle d'évaluation basé sur des relevés spatiaux structurés par âge (SSURBA) est mis au point et utilisé pour le stock des Grands Bancs (divisions 3LNO de l'OPANO) de plies canadiennes (*Hippoglossoides platessoides*) à Terre-Neuve-et-Labrador. Le modèle d'espace d'états est calé sur des indices de relevés par navire de recherche (NR) de l'âge selon la taille du stock qui sont présumés proportionnels à l'abondance. Nous modélisons la capturabilité indexée (q) en tant que fonction logistique de la longueur des poissons, qui varie selon l'âge, la cohorte et le moment du relevé; ainsi le modèle facilite l'estimation de q qui varient dans l'espace et le temps à la suite de changements de la croissance des poissons et des engins utilisés pour les relevés. Le modèle SSURBA produit des estimations au niveau de la division des taux de mortalité par pêche (F), de la productivité du stock et de la taille du stock au vu de l'hypothèse de capturabilité logistique pour $q = 1$ pour des âges entièrement sélectionnés. Le modèle spatial nous permet d'inclure plus d'information tirée des relevés que ce que permet le modèle d'évaluation spatialement regroupé (ensemble des 3LNO) actuellement utilisé pour évaluer l'état du stock. Le modèle peut fournir des estimations des prises relatives que nous comparons aux tendances des prises rapportées afin de valider partiellement le modèle. [Traduit par la Rédaction]

Introduction

Canadian fisheries management has a long history of conducting scientific surveys to monitor fish populations, with some of the earliest surveys dating back to the 1970s (Halliday and Fanning 2006; Smith 1970). Indices from these surveys are expected to provide unbiased and reliable information about species abundance and length or age composition because these data are collected using standardized sampling procedures (Legault 2011; Rago 2005). Fisheries-dependent data such as landings (tonnage) and length or age structure provide detailed information on removals from the stock, thereby allowing the provision of catch advice on an absolute scale (Cook 1997). However, these data are more prone to error or bias originating from various aspects related to misreporting of fisheries catch or changes in fishing technology (Pennino et al. 2016). Unreported catch and discards create a discrepancy between fish landings used in an assessment model and the actual at-sea fish removals, thereby biasing stock size estimates (Beare et al. 2005). When fisheries catch rates are used to inform stock trends, many factors that cause changes in fisheries catchability can distort or misrepresent the real trends (Harley et al. 2001; Maunder et al. 2006). A state-of-the-art stock assessment model relies on both these sources of information, the fisheries-independent and -dependent, to describe the stock population dynamics and provide management advice.

The survey-based assessment (SURBA) model is based on a relatively less common approach of using fisheries-independent data alone when there is a lack of reliable catch information (Cadigan 2010; Cook 1997, 2013; Needle 2002). SURBA fits indices of abundance and estimates stock status on a relative scale (relative to the assumed catchability of the survey gear) and provides information on fishing mortality on an absolute scale. Though SURBA is unable to provide advice on catch in absolute terms, it can provide some ideas about historical catch trends. One of the first applications of the SURBA model was to the six major fish stocks of the North Sea (Cook 1997). Since then, SURBA has been applied to the International Council for the Exploration of the Sea (ICES) assessments of several demersal stocks (Beare et al. 2005; Needle 2002) and to assessments of the cod stocks in Northwest Atlantic Fisheries Organization (NAFO) Divisions 2J3KL (DFO 2013) and Subdivision 3Ps (Cadigan 2010; DFO 2019).

Received 5 December 2019. Accepted 16 June 2020.

R. Kumar,* N.G. Cadigan, and N. Zheng. Centre for Fisheries Ecosystems Research, Fisheries and Marine Institute, Memorial University of Newfoundland, P.O. Box 4920, St. John's, NL A1C 5R3, Canada.
D.A. Varkey and M.J. Morgan. Fisheries and Oceans Canada, Northwest Atlantic Fisheries Centre, P.O. Box 5667, St. John's, NL A1C 5X1, Canada.
Corresponding author: Rajeev Kumar (email: Rajeev.Kumar@dfo-mpo.gc.ca).
*Present address: Fisheries and Oceans Canada, Northwest Atlantic Fisheries Centre, P.O. Box 5667, St. John's, NL A1C 5X1, Canada.

Fig. 1. Study area: the boundaries for NAFO management divisions and the Canadian Exclusive Economic Zone (EEZ) of 200 nautical miles (1 n.mi. = 1.852 km) are illustrated by the solid and dotted lines, respectively. Grey-scale shades distinguish bathymetry ranges. Divisions 3LNO constitute the Grand Banks stock of American plaice. Areas outside the EEZs are NAFO's Regulatory Area (NRA). We use "PBSmapping" package (Schnute et al. 2019) in R to render this map using topography data from Smith and Sandwell (1997), divisions boundaries data from NAFO, and EEZs data from the Fisheries and Oceans Canada (DFO).

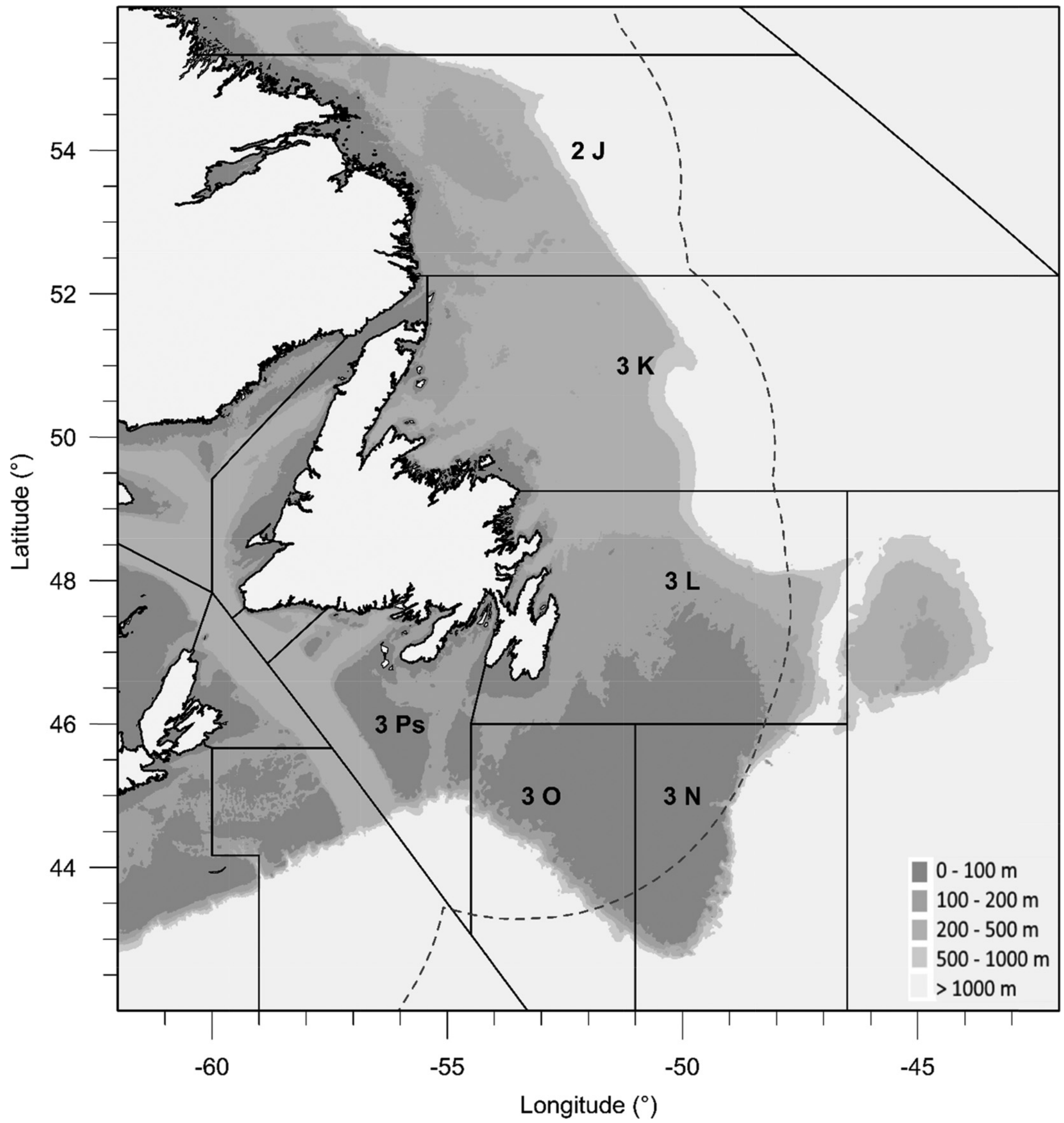

Our present work on a state-space spatial SURBA (i.e., SSURBA) model is applied to the Grand Banks stock of American plaice (*Hippoglossoides platessoides*). The stock covers a large area and extends over three NAFO divisions (i.e., 3L, 3N, and 3O, which we refer to as 3LNO in this paper; Fig. 1). The stock is monitored mainly using indices of abundance obtained from the Canadian Research Vessel (RV) bi-annual bottom trawl surveys that consistently follow a stratified-random sampling design (Doubleday 1981; Smith 1996). The survey data indicate some differences in age composition among the three NAFO divisions (Fig. 2); in particular, in recent years there are differences in abundance trends of prerecruits (ages < 5) in Division 3L and Divisions 3NO (Fig. 2; Kumar et al. 2019; Wheeland et al. 2018). Additionally, previous and ongoing work suggests that American plaice in the three divisions have different growth patterns (Perreault et al. 2019; Zheng et al. 2020). To address these heterogeneities in productivity processes among the three NAFO divisions, we introduce spatial components to the SURBA model.

The American plaice fishery has been one of the largest flatfish fisheries in the world (DFO 2011) that landed as much as over 94 000 tonnes (t) in 1967 (Wheeland et al. 2018). However, by the mid-1990s, the population declined by nearly 90% from historical levels, and therefore a moratorium on directed commercial fisheries was enforced in 1995 (Busby et al. 2007). Since then American plaice are caught as bycatch. Although it has been difficult to obtain "precise estimates" of the bycatch (Wheeland et al. 2018), the average landings after the moratorium is about 1500 t·year^{-1}. Estimates of unintended removals for fisheries under moratorium are commonly "unavailable or unreliable" (Petitgas et al. 2009). The limited reliability of the bycatch records is an important motivation for us to develop a "catch-free" SSURBA model. Further, our rationale for developing SSURBA is that reliable fisheries landings and age composition information will not usually exist at the spatial scales of interest, whereas the survey information will. SSURBA can be considered a first step towards develop-

Fig. 2. Indices of abundance: the figure shows the spatiotemporal coverage of the Canadian fall and spring surveys in the NAFO Divisons 3LNO and Spanish spring survey in the NRA of 3N. The size of bubbles is proportional to the size of indices. Historically, the Canadian research vessel (RV) surveys have used three different sampling trawls; the three shades of bubbles differentiate indices obtained from these trawls.

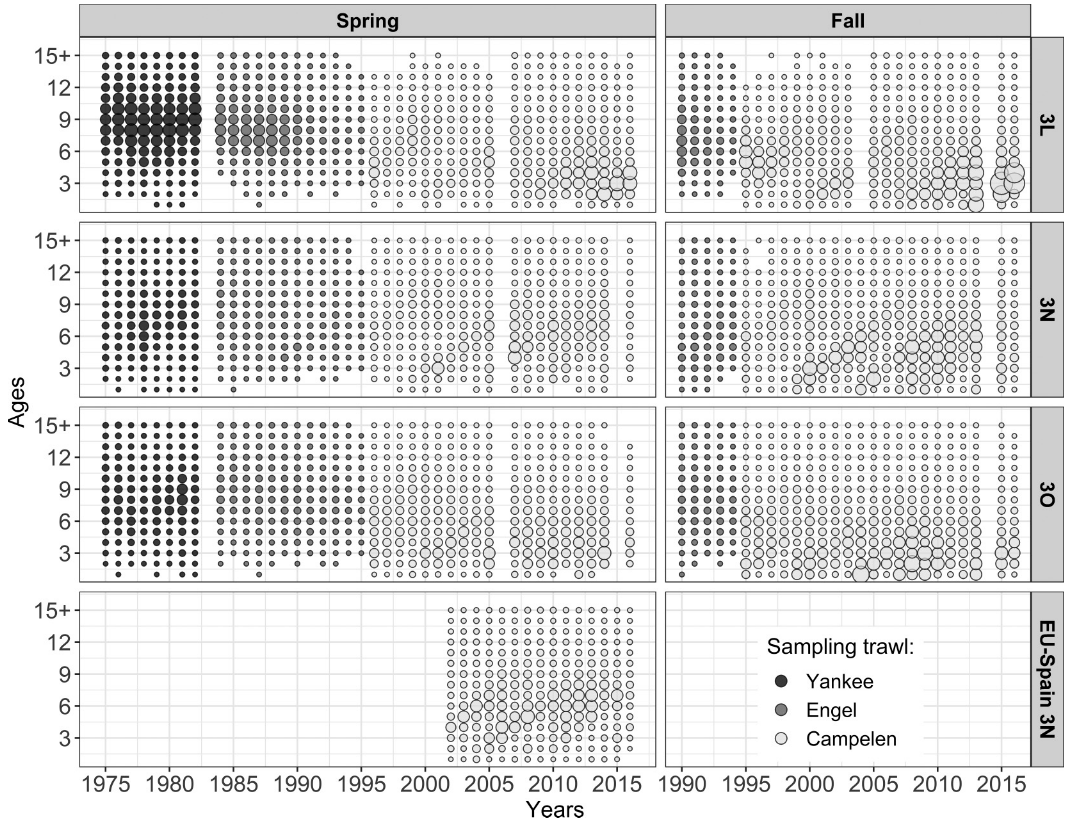

ing an integrated spatial state-space stock assessment model, particularly in situations where good survey data are available.

The SSURBA accounts for spatial differences in recruitment, growth, and fishing mortality and therefore creates a more realistic representation of stock population dynamics and generates information for spatial management questions. The SSURBA method is presented not as an alternative to a standard advanced stock assessment model but as an approach to "fill the gap" (Cook 2013) for methods to use when catch information is unreliable or unavailable, but survey catch (indices of abundance) with adequate temporal and spatial coverage are available. Currently, all the three divisions of the stock are assessed collectively using a virtual population analysis (VPA) with the ADAPTive framework (Gavaris 1988), which we refer to hereinafter as "VPA-ADAPT" or simply "ADAPT", and the assessment suggests that the stock continues to be below the B_{lim} of 50 000 t, in spite of small fishery removals (Wheeland et al. 2018). Retrospective patterns in the ADAPT suggest that biomass is overestimated and fishing mortality is underestimated. The ADAPT model relies heavily on the catch-at-age data (Butterworth and Rademeyer 2008) from the small and uncertain estimates of the bycatch fisheries to reconstruct the population abundance. Furthermore, ADAPT assumes that most of the error is in the index data (Mayo 2003) and works best when fishing mortality is higher than natural mortality (Methot and Wetzel 2013). We investigate whether our SSURBA model provides similar estimate of current stock status compared with that of NAFO assessment. We are also able to utilize additional historical survey indices (prior to 1985) that are not used in the ADAPT model. We also expect that the SSURBA model will be able to separate the signals in abundance changes in the three divisions and be able to inform spatial management questions. We provide comparisons between stock trends obtained from SSURBA and the ADAPT assessment and between predicted landings from SSURBA and reported landings.

Methods

Data

The primary data used in the model are indices of abundance from the Canadian RV surveys in NAFO Divisions 3LNO (the Grand Banks) and from EU–Spanish RV surveys in the NAFO Regulatory Area (NRA) of Division 3N (Fig. 1). These surveys use bottom otter trawls and follow a depth-stratified random sampling protocol.

The ongoing Canadian RV surveys sample the divisions twice in a year: April to July in the spring and October to usually mid-December in the fall (Power et al. 2015). Spring surveys started in 1975, while the fall surveys started in 1990. Two major changes in the survey gears occurred since 1975. From 1975 to 1982, the surveys were conducted with the RV *AT Cameron* using a Yankee 41.5 otter trawl. In 1983, the Engel 145 hi-lift bottom trawl used with the RV *Wilfred Templeman* replaced the Yankee trawl and continued sampling until spring 1995. A comparative fishing experiment between the two gears was commissioned by Fisheries and Oceans Canada, and the Yankee time series were converted to Engel equivalents, producing a single Engel series running from 1975 until spring 1995. From the fall 1995 survey, the Campelen 1800 shrimp trawl, used with the RVs *Alfred Needler* and *Teleost* in the fall and mainly by the RV *Teleost* in the spring, replaced the much bigger mesh-sized Engel 145 bottom trawl. The surveys have been conducted with the same gear and vessels since then (Power et al. 2015). Mesh size for the Campelen trawl varies from 80 mm near the wings to 40 mm near the lower bellies and cod end compared with that of the Engel's 180 mm near the wings to 130 mm near the lower bellies and cod end; clearly, the differences

Table 1. Data used in the model.

Data type			Description
1. Indices			Used to fit the observation model
Trawls	Spring	Fall	
Yankee	1975–1982	NA	
Engel	1984–1995	1990–1994	
Campelen	1996–2016 (except 2006, 2014 (in 3NO))	1995–2016 (except 2004 (in 3L), 2014)	
EU–Spanish Campelen (3N of NRA only)	2002–2016 (except 2006)	NA	
2. Division-wise length-at-age from 1978 to 2015			Used to estimate growth parameters
3. Division-wise weight-at-length			Used to convert length-at-age to weight-at-age for biomass and SSB calculation
4. Division-wise maturity-at-age from 1975 to 2016			Used to calculate SSB from biomass

in mesh sizes make considerable differences in catchabilities of both the gears (McCallum and Walsh 1996). Apart from the variations in mesh size, the sampling protocols for both gears were different in terms of sampling time, towing speed, and swept-area covered (McCallum and Walsh 1996); therefore, indices of abundance obtained by the Campelen and Engel surveys are not directly comparable. To make both the data series comparable, a set of length-based conversion factors (CF) was derived through a number of comparative fishing trials in 1996 (Morgan et al. 1998; Warren et al. 1997).

The EU–Spanish survey in the 3NO NRA is conducted in the spring (typically from June to July) of each year by the RV *Vizconde de Eza* using the Campelen 1800 shrimp trawl, which has similar construction to the Canadian version of the Campelen 1800 shrimp trawl but uses much longer sweep lines (Walsh et al. 2001). Since the sampling area of the NRA of Division 3O is very small, we only use the 3N survey (but not 3O survey) from 2002 to 2016 in the analysis.

In summary, in our stock assessment model, we use spatial age-structured Engel-equivalent indices of abundance from the Yankee trawl survey running from 1975 to 1982, Engel survey indices from 1984 to the spring of 1995, Campelen survey indices from the fall of 1995 to 2016, and EU–Spanish survey indices from 2002 to 2016 (total data of 42 years from 1975 to 2016; Fig. 2). We also use the findings from the comparative fishing experiments, between the Engel and Canadian Campelen surveys, to adjust for the differences in catchabilities between the two surveys. The other data incorporated in the model are spatiotemporal length-at-age, weight-at-length, and maturity-at-age for American plaice derived from the RV surveys. The length-at-age is used to convert length-based catchabilities to age-based ones when fitting the Campelen and Engel survey indices. Further, length-at-age along with length–weight and maturity-at-age are used in the computation of biomass and spawning stock biomass. A complete list of the data we used in this study is provided in Table 1.

Model

A fisheries state-space model typically comprises a state equation with random-effect process error(s) that describes the unobserved state of the population (process model) and an observation equation with observation or sampling errors that relates the observed data to the underlying state dynamics (observation model; de Valpine 2002; Nielsen and Berg 2014). The two errors add stochasticity in the model at two levels: the process error represents uncertainties in the state or process caused by natural variation, such as changes in the physiological responses of the population to environmental fluctuations, and observation error accounts for the variability in the data caused by sampling variation (Maunder and Piner 2014; Newman et al. 2014).

Process model and components

The key objective of our SSURBA model is to estimate the relative abundance-at-age for the time period of the survey indices of abundance. In the age-structured population process, a cohort's abundance-at-age is tracked using the standard exponential-decay model, where N number of fish of age a at the start of year y in division d and their respective per-year instantaneous rate of total mortality Z, which is the sum of natural mortality rate M and fishing mortality rate F, predicts the population in the next year (eq. 1):

$$(1)\qquad N_{a+1,y+1,d} = N_{a,y,d}\exp(-F_{a,y,d} - M_{a,y,d}),\\ a = 1,\ldots,A-1;\quad y = 1,\ldots,Y-1;\quad d = 1,\ldots,D$$

The last age ($a = A$) in the population model (eq. 1) is the "plus group" that contains the population of age 15 and older fish (15+). The plus group population in year y is obtained by the addition of plus group survivors of the previous year ($y - 1$) to the population of age 15 fish in the year y (eq. 2). The plus group population at first year ($N_{15+,1,d}$) is one of the model parameters to be estimated.

$$(2)\qquad N_{15+,y,d} = N_{15+,y-1,d}\exp(-Z_{15+,y-1,d}) + N_{14,y-1,d}\exp(-Z_{14,y-1,d})$$

In this paper we do not consider the species movement between divisions; this decision is based on tagging studies conducted on juvenile and adult American plaice on the Grand Banks, which do not suggest that the species moves or migrates over large distances (Morgan 1996). On average, fish were recovered within ~34–52 nautical miles (1 n.mi. = 1.852 km) of release sites, which is a small distance in comparison with the large areas encompassed by the divisions. We further discuss the implications of this assumption in the Discussion section.

Fishing mortality rate (F)

In our model, stochasticity is not included directly in the state equation but in the parameterization of F. Consistent with the accepted assessment of this stock (Wheeland et al. 2018), we assume no commercial catch for the ages 1 to 4, so we have fixed F to be zero for these younger ages. For older ages (age ≥ 5), the logarithm of $F_{a,y,d}$ in eq. 1 follows a mixed-effects model with mean $\log(\mu_{y,d})$, within division age–year random deviations $\Delta_{a,y,d}$ and between divisions spatiotemporal random deviations $\lambda_{y,d}$ (eq. 3). We constrain values of $\mu_{y,d}$ to two values representing pre- and postmoratorium years in each division, so there are only six mean F parameters in the model. Estimating separate means for the two periods accounts for the drastic change in F that resulted from the moratorium.

$$F_{a,y,d} = \mu_{y,d} \exp(\Delta_{a,y,d} + \lambda_{y,d}), \quad a = 5, \ldots, A \tag{3}$$

In each division (d), the temporal component (age and year) follows a multivariate normal (MVN) distribution with mean 0 and covariance matrix $\boldsymbol{\Sigma}_\Delta$. We assume separable first-order autoregressive (AR1) models for both the age and year; therefore, elements of $\boldsymbol{\Sigma}_\Delta$ are based on

$$\begin{aligned} \mathrm{Cov}(\Delta_{a,y,d}, \Delta_{a-m,y-n,d}) &= \frac{\sigma^2_{\Delta,d}\phi_A^{|m|}\phi_Y^{|n|}}{\left(1-\phi_A^2\right)\left(1-\phi_Y^2\right)} \\ \mathrm{corr}(\Delta_{a,y,d}, \Delta_{a-m,y-n,d}) &= \phi_A^{|m|}\phi_Y^{|n|} \end{aligned} \tag{4}$$

where, ϕ_A and ϕ_Y are the age and year autocorrelation coefficients, respectively. We assume all $\Delta_{a,y,d}$ and $\Delta_{a'y'd'}$ are independent if $d \neq d'$.

The between-division correlation in F is modeled through λ, where $\boldsymbol{\lambda}_y = (\lambda_{y1}, \ldots, \lambda_{yD})^T$ and follows an MVN distribution, $\boldsymbol{\lambda}_y \sim \mathrm{MVN}^{D\times D}(0, \boldsymbol{\Sigma}_\lambda)$, where the dimension $D = 3$ is the total number of divisions. An element of $\boldsymbol{\Sigma}_\lambda$ between any two divisions is equal to the product of correlation r_λ between them and their respective standard deviations σ_λ, as shown in eq. 5:

$$\boldsymbol{\Sigma}^D_{\lambda,d_i,d_j} = r^D_{\lambda,d_i,d_j} \times \sigma_{\lambda,d_i} \times \sigma_{\lambda,d_j}, \quad \boldsymbol{\Sigma}_{\lambda,d_i,d_j} = \sigma^2_{\lambda,d_i} \quad \text{for } i = j \tag{5}$$

We explore two variants of the F model: with and without the divisional correlation λ in eq. 3 and compare the fits using the Akaike information criterion (AIC).

Natural mortality rate (M)

There is ample research on the relationship between fish size and natural mortality with smaller sized fish having higher M than the larger ones (Lorenzen 1996; Miller and Hyun 2017; Peterson and Wroblewski 1984). This implies that growth may be a proxy for many factors driving natural mortality. In this work, we assume an empirical relationship between M and fish weight (W) as $\log(M) = b - 0.305 \log(W)$ based on Miller and Hyun (2017). We model weight as a power function of length (L) and therefore reformulate the equation for M as

$$M_{a,y,d} = \exp(b_d)(\alpha_d L_{a,y,d})^{-\beta_d \times 0.305} \tag{6}$$

where L is length, α and β are the parameters of the weight-at-length model fitted separately for each division (refer to online Supplementary material, Fig. S1[1]), and the value −0.305 is an allometric scaling factor commonly used in the oceanic environment (Lorenzen 1996). The value for the scaling component b is derived by setting M for the maximum length of the plus group (age 15+) equal to 0.05 in eq. 6 and solving for b (eq. 7):

$$b = \log(0.05) + 0.305 \log[\max(W)] \tag{7}$$

where $\max(W)$ is the corresponding weight of the maximum plus group length. Hoenig (1983) proposed a regression method to estimate M based on data from 134 stocks of 79 species of fish. This regression equation roughly equates to 1.5% of the stock surviving to the oldest age of fish for the stock (Hewitt and Hoenig 2005). We fix the value of M for the plus group (age 15+) at 0.05 to approximate this assumption. Since fish lengths-at-age vary over cohort and division (Fig. S2[1]), this formulation allows spatiotemporal variation in M (Fig. A1).

Length-at-age in eq. 6 has been estimated from a spatiotemporal biphasic (separate for immature and mature fish) von Bertalanffy growth model applied to length-at-age data obtained from the Canadian RV surveys in Divisions 3LNO (Fig. S2[1]). Age samples are collected using a length-stratified sampling design that may introduce bias in the estimation of von Bertalanffy growth parameters (Perreault et al. 2019). The growth model and estimation methods that account for the length-stratified sampling design and other issues are described in the recent publication by Zheng et al. (2020).

Recruitment (R)

Similar to F, the numbers of recruits at age 1 (R) are estimated by a stochastic process about a mean recruitment (μ_R). The logarithm of R follows a mixed-effect model with mean $\log(\mu_R)$ and a normal random deviation (δ) that follows a linear AR(1) process with autocorrelation ϕ_R and error e (eqs. 8 and 9). Spatial correlation between divisions is modelled through the vector of errors, $\boldsymbol{e}_y = (e_{1,y}, \ldots, e_{D,y})$ that follows a D-dimensional MVN distribution with mean 0 and a covariance matrix $\boldsymbol{\Sigma}_R$ (eq. 9).

$$R_{y,d} = \mu_{R,d} \exp(\delta_{y,d}); \quad \delta_{y,d} \sim \mathrm{AR}(1) \tag{8}$$

$$\delta_{y,d} = \phi_{R,d}\delta_{(y-1),d} + e_{y,d}; \quad \boldsymbol{e}_y \sim \mathrm{MVN}^{D\times D}(0, \boldsymbol{\Sigma}_R) \tag{9}$$

Elements of $\boldsymbol{\Sigma}_R$ are defined as a product of correlation (ρ_R) between the divisions and their respective standard deviations σ_R; the calculation is similar to what is shown in eq. 5. However, since this is a stationary AR(1) process (i.e., $-1 < \phi_R < 1$), the marginal divisional correlation (ρ'_R) and AR(1) standard deviation (σ'_R) for the first year are defined as

$$\rho'_{R,d_i,d_j} = \rho_{R,d_i,d_j}\frac{\sqrt{1-\phi^2_{R,d_i}}\sqrt{1-\phi^2_{R,d_j}}}{1-\phi_{R,d_i}\phi_{R,d_j}} \tag{10}$$

$$\sigma'_{R,d} = \frac{\sigma_{R,d}}{\sqrt{1-\phi^2_d}} \tag{11}$$

Observation model and components

The observation model relates the observed and predicted indices of abundance. Let $\hat{I}_{a,y,s,d}$ denote the predicted indices of age a in year y, survey s (Canadian fall, Canadian spring, and EU–Spanish), and division d. The model parameters are estimated by fitting the observed indices $I_{a,y,s,d}$, obtained from the Canadian spring and fall survey (s) in the NAFO Divisions 3LNO and EU–Spanish spring survey in NRA 3N, to the $\hat{I}_{a,y,s,d}$ in the observation model (eq. 12), where the observation error (ϵ) is normally distributed with mean 0 and allowed to have a different variance σ_I for smaller ages ($a \le 5$) because these younger ages may not be fully selected by the survey gears and could have higher variance than fully selected older fish.

$$I_{a,y,s,d} = \hat{I}_{a,y,s,d} \times \exp(\epsilon_{a,y,s,d}), \quad \epsilon_{a,y,s,d} \sim N\left[0, \begin{cases} \sigma_{I1}, & \text{if age} \le 5 \\ \sigma_{I2}, & \text{if age} > 5 \end{cases}\right] \tag{12}$$

The $\hat{I}_{a,y,s,d}$ in eq. 12 is computed by using the survey-gear catchability (q), population abundance (N), and additional accounting for Z from the beginning of the year to the time of survey (f_s) (eq. 13):

$$\hat{I}_{a,y,s,d} = \frac{q_{a,y,s,d} \times N_{a,y,d} \times \exp(-Z_{a,y,d} \times f_s)}{\mathrm{SAR}}, \quad \mathrm{SAR} = \begin{cases} 1.83, & \text{if Engel} \\ 1.0, & \text{otherwise} \end{cases} \tag{13}$$

[1]Supplementary data are available with the article through the journal Web site at http://nrcresearchpress.com/doi/suppl/10.1139/cjfas-2019-0427.

Since the area swept by the two Canadian sampling gears, Engel and Campelen, are different, we account for the differences by dividing the eq. 13 with 1.83, which is the swept area ratio (SAR) of Engel to Campelen (Morgan et al. 1998). Together, the SAR and the use of catchability ratio between Engel and Canadian Campelen gears (explained in the following section) allow the treatment of the entire length of Canadian RV spring and fall surveys as unique uninterrupted time series of indices in the model. To avoid a potential confusion, we clarify that EU–Spanish gear are modelled with independent catchability, and the SAR-based adjustment is only applied to the Canadian RV survey series.

The q term in eq. 13 differs depending on the type of trawls used for the sampling. We model q of all the three sampling gears (g) separately as a logistic function of mean length with logistic parameters $L95$ (length at 95% catchability) and $L50$ (length at 50% catchability) (eq. 14). Mean length L in eq. 14 is a function of age (adjusted to the timing of survey s) determined by the combination of growth parameters specific to cohort (c) and division (d). Formulating the model this way makes q change with age, year, and survey (fall and spring) for each division. The details about the method to estimate the spatiotemporal growth parameters are available in Zheng et al. (2020). Since the survey coverage area for EU–Spanish survey is small compared with that of Canadian survey, we multiply eq. 14 by an additional scaling factor (Ω) for the q of EU–Spanish survey, where Ω is one of the parameters to be estimated.

$$(14) \qquad q_g = \frac{1}{1 + \exp\left[\frac{\log(19)}{L95_g - L50_g} \times (L50_g - L_{c,s,d})\right]}$$

As mentioned in the Introduction section, the Canadian surveys have used different trawls with different q values in the modelled time period. Comparative fishing trials were performed in the mid-1990s with an aim to estimate length-based CF for Engel survey catches to Campelen equivalents by fitting a model to the ratio of the number of fish caught in the Campelen to that of Engel against fish length (Morgan et al. 1998; Warren et al. 1997). The CF was not well defined for fish smaller than 23 cm mainly because of very small sample size for fish in this length range caught by the Engel trawl, and CF for fish greater than 40 cm was approximately equal to 1. The CF for fish lengths 25–40 cm was well defined, and we have used the CF for this length range as a prior in our model. Thus, parameters $L50$ and $L95$ are estimated freely for Engel and Campelen gears, but the catchability ratio of Canadian Campelen to Engel ($q_{\mathrm{Campelen}}/q_{\mathrm{Engel}}$) for the length ($25 < L < 40$) are linked to the CF through a gamma distribution:

$$(15) \qquad \frac{q_{\mathrm{Campelen}}}{q_{\mathrm{Engel}}} \sim \mathrm{Gamma}(k, \theta_L)$$

where shape $k = 1/\mathrm{CV}^2$, scale $\theta_L = \mu_L \times \mathrm{CV}^2$, and μ_L (for $25 < L < 40$) follows the relationship formulated in Morgan et al. (1998) as shown in eq. 16:

$$(16) \qquad \mu_L = \exp\{39.96 + 0.36[L - 41\log(L)]\}$$

Since a variance estimate for the CF was not available, we have estimated the coefficient of variance (CV) based on the residuals for the model fit in Warren et al. (1997).

Parameters estimation

The cohort population dynamic model (eq. 1) requires the estimation of the following parameters: (i) the components of recruitment: mean recruitment $\mu_{R,d}$ and recruitment deviation $\delta_{y,d}$ of 1-year-old fish, (ii) age-wise abundance of fish in the first year $N_{a,1,d}$, and (iii) the components of F: mean $\mu_{y,d}$, separable AR deviation $\Delta_{a,y,d}$, and spatial year effects $\lambda_{y,d}$. Recall that we do not estimate the matrix of M as model parameters; instead, we compute M using eqs. 6 and 7 and provide it to the model for the calculation of $\mathbf{Z}$ matrix. We also estimate logistic catchability parameters $L50_g$ and $L95_g$ for all the survey gears. Other parameters include various model variances, autocorrelation parameters in the estimation of R and F deviations, and parameters for various covariance matrices. A full list of model parameters, notations, and symbols are summarized in Table 2.

Objective function

We use the TMB package (Kristensen et al. 2016) in R (R Core Team 2019) for the implementation of the models. Parameters are estimated using the maximum likelihood approach (MLE), where the –log likelihood function (objective function) is minimized using the "nlminb" optimization function of R. Recruitment deviations $\delta_{y,d}$, separable AR deviations $\Delta_{a,y,d}$, and spatial year effects $\lambda_{y,d}$ of F are estimated as random-effect parameters, which means that the marginal likelihood of data are computed by "integrating out" the random effects from the joint likelihood over their assumed distribution (Kristensen et al. 2016). TMB uses Laplace approximation for the estimation of integrals over the high-dimensional random effects. TMB also provides the "SEPARABLE" function to compute the separable extension of two MVN densities (TMB documentation 2019). We have used this function in the parametrization of F. The objective function to be minimized is the summation of individual –log likelihood (NLL) contributions from the following components: (i) observation error (or data) that follows a normal density, (ii) AR(1) process for correlated recruitment deviations that follows an MVN density, (iii) $\Delta_{a,y,d}$ follows a separable AR(1) process for correlated age–year deviations from mean, (iv) spatial year effects $\lambda_{y,d}$ follows an MVN, and (v) catchability ratio of Campelen to Engel ($q_{\mathrm{Campelen}}/q_{\mathrm{Engel}}$) are linked to conversion factors from comparative fishing through gamma density. In summary, the optimized objective function is the marginal likelihood of the data, obtained after integrating out the unobserved random effects.

As previously described, we explore two F models: with or without divisional correlation (spatial correlation). We select the model that provides the best fit, that is the model with the lowest AIC. We calculate AIC differences (ΔAIC) of models from the model yielding lowest AIC; typically, models with $\Delta\mathrm{AIC} \geq 10$ are thought to be not supported by the data (Mangel 2006) and therefore eliminated from the further discussion.

Results

Based on AIC, the model with F correlated across divisions (model 2) had the best performance (Table 3), and the results presented hereinafter are based on model 2, suggesting that the trends in fishing mortality are similar among the Grand Banks divisions.

We present the modelling results under three broad headings: (i) Model diagnostics, (ii) Parameters estimated, and (iii) Stock performance.

Model diagnostics

Residual analyses and the model fit

Following eq. 12, Pearson standardized residuals are defined as $[\log(I_{a,y,s,d}) - \log(\hat{I}_{a,y,s,d})]/\sigma_I$, with $\sigma_I = \sigma_{I1}$ and σ_{I2} accordingly. The conditional distribution of the residuals given all the random effects is independent standard normal. Hence, if both $\hat{I}_{a,y,s,d}$ and σ_I are estimated accurately, then the residuals should have an independent standard normal distribution, which provides a partial validation of the model and the estimation approach. However, estimation of $\hat{I}_{a,y,s,d}$ involves predictions of random effects, and the predictions may be smoother than the population values. There-

Table 2. Model notations and parameters.

Symbol	Description	Value
D	Total number of divisions	3 (3L, 3N, 3O)
Y	Total number of years	41
A	Plus group age	15+
d	Division index	1, 2, D
y	Year index	1, 2, …, Y
a	Age index	1, 2, …, A
s	Survey	Canadian fall, Canadian spring, EU–Spanish
$N_{a,y,d}$	Population abundance in age a, year y, and division d	
$F_{a,y,d}$	Fishing mortality rate in age a, year y, and division d	
$\mu_{y,d}$	Fixed-effect component of F in year y and division d	
$\Delta_{a,y,d}$	Age–year autocorrelated random deviation in F for division d	
$\lambda_{y,d}$	Division-wise correlated random year effect component in F	
$\mathbf{\Sigma}_{\Delta}$	Stationary covariance matrix of an AR(1) process for the random deviation in F	
$\sigma^2_{\Delta,d}$	Variance for the random deviation in F for division d	
ϕ_A and ϕ_Y	Age and year autocorrelation function in F	
$\mathbf{\Sigma}_{\lambda}$	Covariance matrix for the spatial year effect in F	
$r_{\lambda,d_i d_j}$	Between divisions correlation in F	
$\sigma_{\lambda,d}$	Standard deviation (SD) for the spatial year effects in F for division d	
$M_{a,y,d}$	Natural mortality rate in age a, year y, and division d	
b	A scaling factor in the allometric relation between M and weight	
α and β	Parameters in fish length–weight model	
$L_{a,y,d}$	Length (cm) of fish in age a, year y, and division d	
W	Weight of fish (g)	
$R_{y,d}$	Recruitment of age 1 fish in year y and division d	
$\mu_{R,d}$	Mean recruitment in division d	
$\delta_{y,d}$	Random recruitment deviation in year y and division d	
$\phi_{R,d}$	Autocorrelation in recruitment deviation in division d	
$e_{y,d}$	Error term of AR(1) model for recruitment deviation in year y and division d	
$\mathbf{\Sigma}_R$	Stationary covariance matrix of the error term in random recruitment deviation	
ρ_{R,d_i,d_j}	Between divisions correlation in recruitment	
ρ'_{R,d_i,d_j}	Marginal divisional correlation in recruitment	
$\sigma_{R,d}$	SD of the error term in recruitment deviation in division d	
$\sigma'_{R,d}$	AR(1) SD of the error term in recruitment deviation in division d	
$I_{a,y,s,d}$ and $\hat{I}_{a,y,s,d}$	Observed and predicted indices of abundance for survey s in age a, year y and division d	
ϵ	Observation error	
σ_{I1}	SD of observation error for ages ≤ 5	
σ_{I2}	SD of observation error for ages > 5	
$q_{a,y,s,d}$	Survey gear catchability for age a, year y, in division d	
Ω	Catchability scaling factor for EU–Spanish survey	
f_s	Fraction of the year survey occurred in	
SAR	Swept area ratio of Engel to Campelen survey trawl	
$L50_g$	Mean length at which 50% of fish is captured in survey gear g	
$L95_g$	Mean length at which 95% of fish is captured in survey gear g	
q_{Campelen}	Catchability of Campelen	
q_{Engel}	Catchability of Engel	
k and ΘL	Shape and scale parameter of Gamma distribution for the catchability ratio of Campelen to Engel	
μL	Mean catchability ratio of Campelen to Engel for fish length (L) $25 < L < 40$ based on comparative fishing experiment	

Table 3. Negative log-likelihood (NLL) and Akaike information criterion (AIC) values for the various model fits.

Models	No. of parameters	NLL	Deviance	AIC	ΔAIC = AIC – min(AIC)
No spatial component in F	72	3168.44	6336.88	6480.88	29
Spatially correlated year effect in F	78	3147.936	6295.87	6451.87	0

fore, Pearson residuals here cannot be expected to be independent and have exactly unit variance (Thygesen et al. 2017).

Standardized residuals from the Canadian (spring and fall) and EU–Spanish surveys do not show any obvious systematic patterns, and the residuals are randomly scattered around the zero-line between ±2, which validates the normality assumption in the errors (Figs. A2, A3, A4). In general, the model fits the data well for all the ages across all the divisions and surveys (Figs. 3, 4, 5) except for the age 1, especially in the Canadian spring survey of 3L (Fig. 3), where the model overestimates the indices, which is also noticeable in the plot of residuals against age in Fig. A2. We believe that age 1 fish are very small in spring, and the index perhaps represents only the faster-growing age 1 fish. Compared with 3L, 3N and 3O have better fits for age 1 in the spring; the differences in the fit between divisions can be explained by the divisional difference in growth rate — fishes in 3NO generally have faster growth than those in 3L (Fig. S2[1]).

Fig. 3. Model fitting to the time series of the Canadian spring indices for the three divisions. Predicted line is overlaid over the data (circles) in each division–age grid.

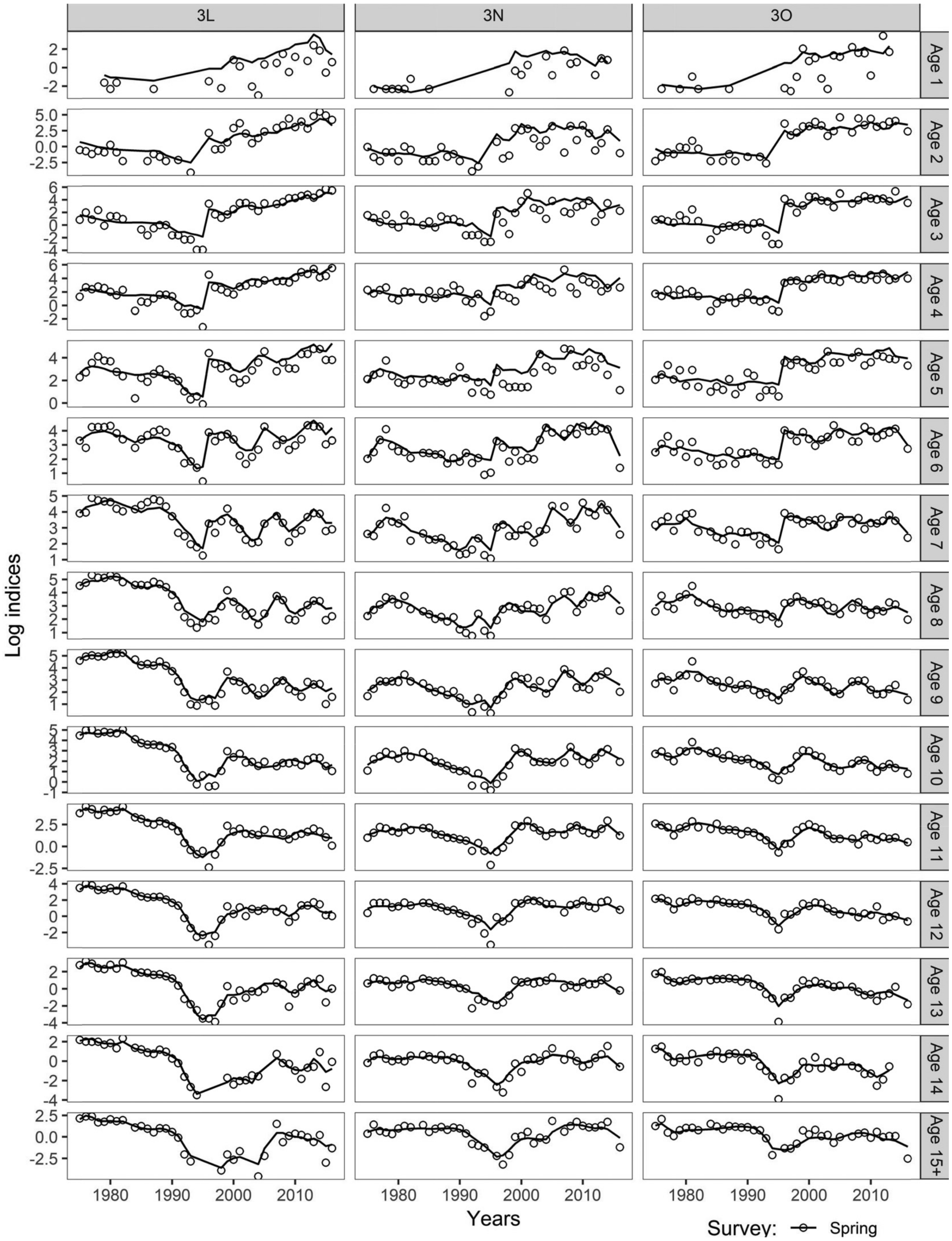

The trends of spring and fall Canadian survey indices are similar, but the difference in magnitude of the indices is conspicuous in the lower ages (Fig. S3[1]). At older ages, fish attain sufficient size to be fully selected and retained in sampling trawls in both the spring and fall surveys. Conversely, at younger ages, there is a considerable difference in catchability due to the difference in fish size between the spring and fall, leading to differences in the magnitude of the index. The length-based parameterization of catchability accounts for this length-at-age difference between spring and fall surveys and therefore produces reasonably good fits to both the survey indices (Figs. 3 and 4).

Retrospective analyses

We perform 6-year retrospective analyses on key model outputs. Retrospective patterns assess whether there is a systematic change in historical estimates of stock size and fishing mortality with the inclusion of data for an additional year. Since the model does not present obvious patterns in the residuals, our expectation is that retrospective patterns will be small. Retrospective patterns are negligible in spawning stock biomass estimates, especially in divisions 3L and 3O, and do not indicate model misspecification (Fig. 6). There is a small retrospective pattern in the SSB estimates for 3N. For the 2014 assessment year, the estimate of

Fig. 4. Model fitting to the time series of the Canadian fall indices for the three divisions. Predicted line is overlaid over the data (circles) in each division–age grid.

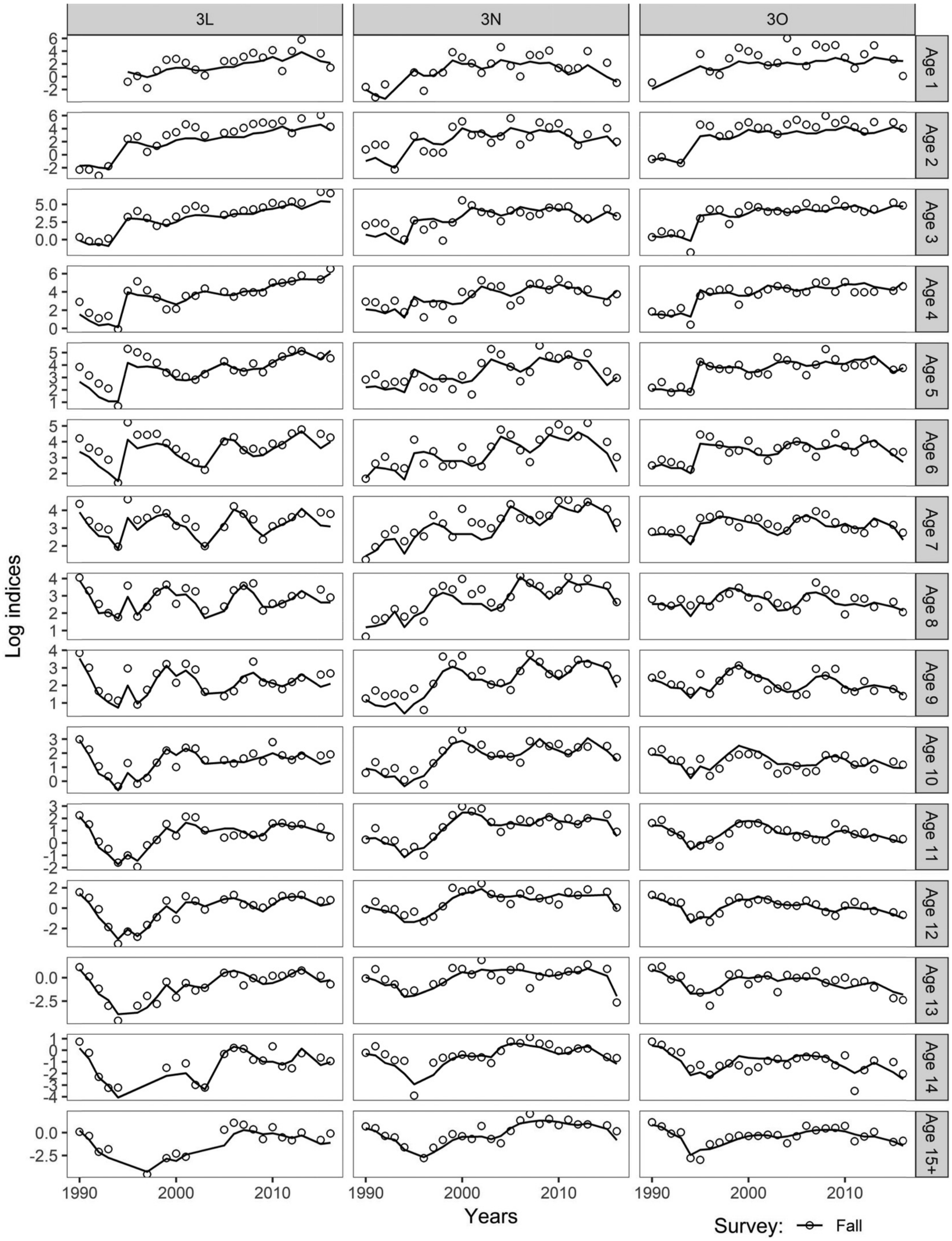

F is small but is revised high for 2015 and 2016 assessment years (Fig. 7). Apart from the estimation for 2014, retrospective patterns in F are small but generally positive and more prominent in 3N. Note that in 2014, the Canadian fall surveys are missed in all the three divisions, and in 2015, the Canadian spring survey is available only for 3L. We consider the retrospective pattern to be good, especially considering that the model is fitted without fisheries data and has limited information to determine F.

All variances

All the standard deviations (SDs) estimated in the model are presented in Fig. 8 and Table S1[1]. The SD for separable model of F deviation ($\Delta_{a,y,d}$; eq. 3) in 3N is about 1.0, which is almost double than that of 3L and 3O, indicating considerable interannual fluctuations or age-specific selectivity fluctuations in fishing mortality in 3N. The spatial correlation component in F ($\lambda_{y,d}$) shows the smallest MVN SD estimate for 3O, followed by 3N and 3L. This indicates that the magnitude of spatially correlated year effects in F is higher in 3L compared with the other two divisions.

The multivariate SDs for recruitment have similar estimates for 3L and 3N (0.6 to 0.7), while the estimate for 3O (0.38) is much smaller than the estimates for 3LN.

The SD for observation error is higher (almost double) for young fish (ages ≤ 5) compared with the older age groups (age 6+). Age-

Fig. 5. Model fitting to the time series of the Spanish survey indices for NRA of Division 3N. Predicted line is overlaid over the data (circles) for each age.

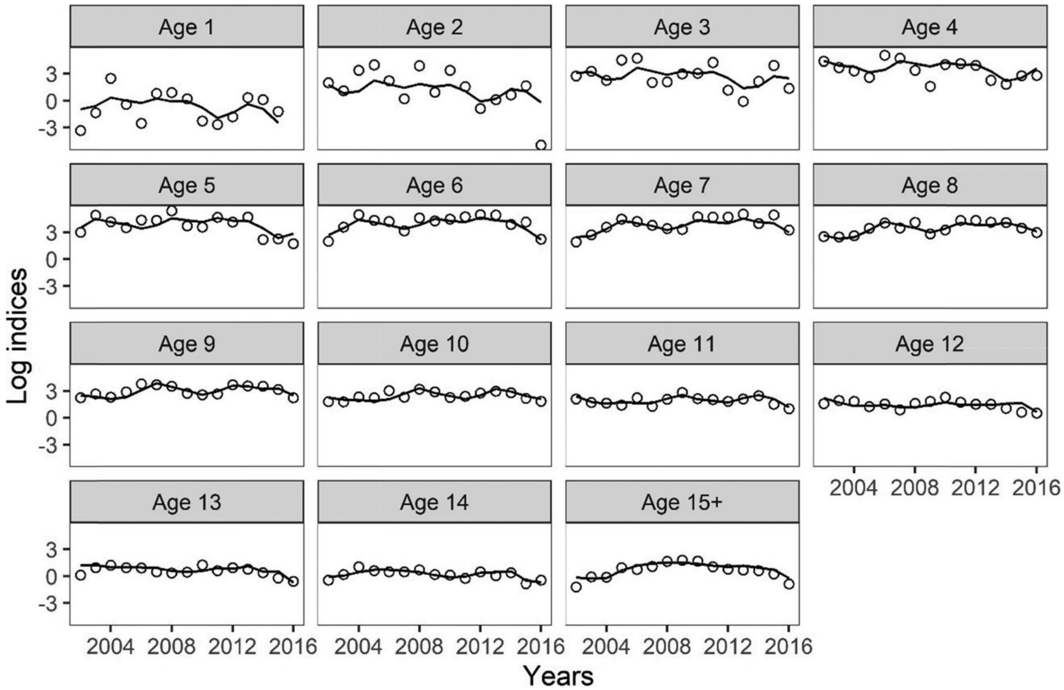

Fig. 6. Spatial retrospective analysis shows the changes in relative spawning stock biomass (SSB) in Divisions 3LNO with each additional year of data used from 2010 to 2016. Circles mark the corresponding retrospective years.

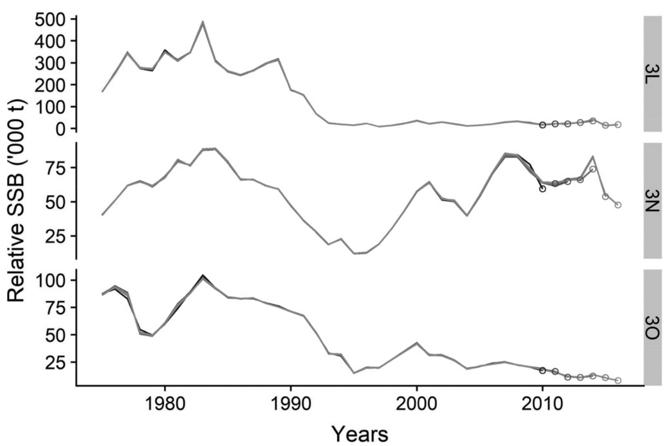

Fig. 7. Spatial retrospective analysis shows the changes in instantaneous rate of fishing mortality (*F*) in Divisions 3LNO with each additional year of data used from 2010 to 2016. Circles mark the corresponding retrospective years.

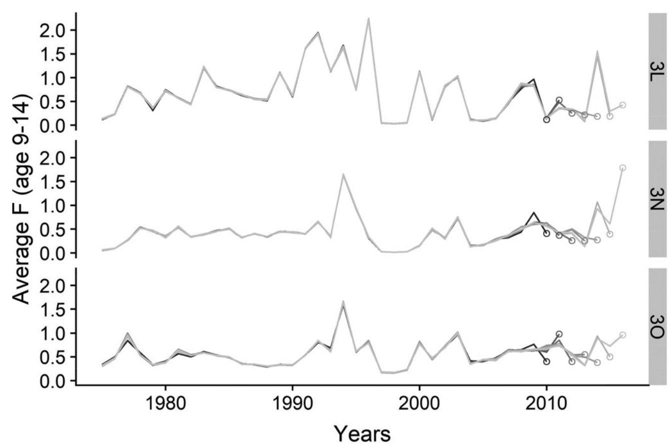

specific selectivity to survey gear varies considerably for the ages 1–5 from year to year and between seasons, and this is the likely reason for higher observation error SD for these ages; with an increase in fish size, the range for catchability variation becomes smaller for older ages (age 6+).

Parameters estimated

First year's abundance-at-age and recruitment

The magnitude of estimated numbers-at-age in the first year ($N_{a,1}$) in 3L is much higher than that in 3NO; $N_{a,1}$ in 3L ranges from ~23 000 million for age 1 to ~16 million for the plus group (15+) (Fig. A5). $N_{a,1}$ in 3O ranges from ~2500 million for age 1 to ~8 million for age 15+, which are mostly higher than the corresponding values in 3N (~2300 million for age 1 to ~3 million for age 15+). Division 3L encompasses a larger area compared with divisions 3N and 3O, and the results show that in the beginning, a larger proportion of the stock is typically in 3L.

Division 3L is the largest contributor to recruitment in the stock; average relative recruitments are estimated as (in million) ~3000, 500, and 700 respectively in Divisions 3LNO (Fig. 9). Multivariate correlation shows that all the divisions are highly correlated (0.74–0.95), with 3N and 3O being the most correlated (Fig. A6). Age 1 recruits declined sharply until the mid-1980s, improved somewhat for a few years, but then further declined in the late 1980s and early 1990s. Since then, recruitment has been more or less stable, mostly below average, in all the three divisions. It is worth mentioning that the fit of age 1 indices shows an increasing pattern (Figs. 3 and 4), while the recruit estimates here do not. The increase in the indices is mainly due to the shift in catchability between the Engel and Campelen survey gears. More age 1 fish were caught by the Campelen trawl (Fig. 2), which has much

Fig. 8. All the variances estimated in the model.

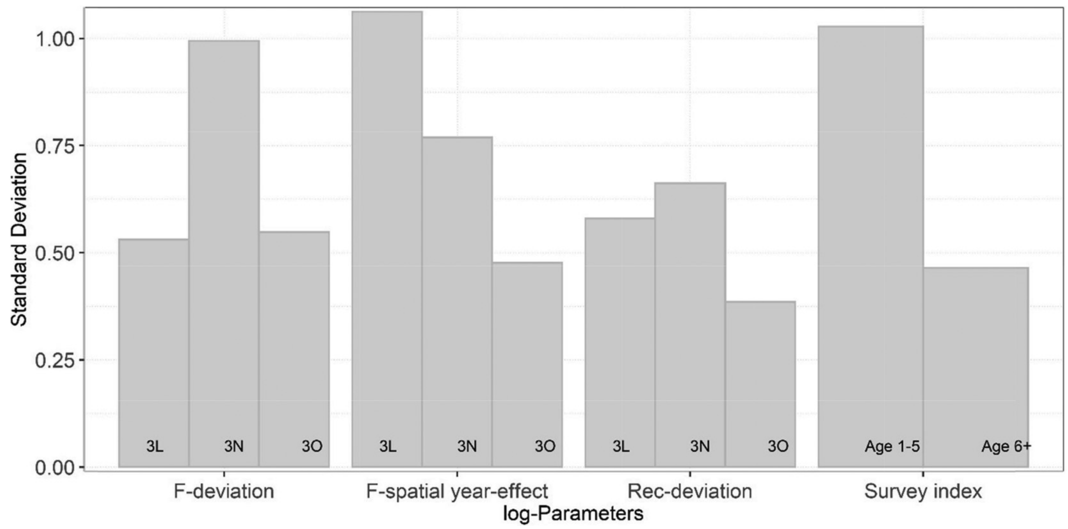

Fig. 9. Relative recruitment across the three Divisions 3LNO with the shading of 95% confidence interval. Dotted line in each division shows the average recruitment.

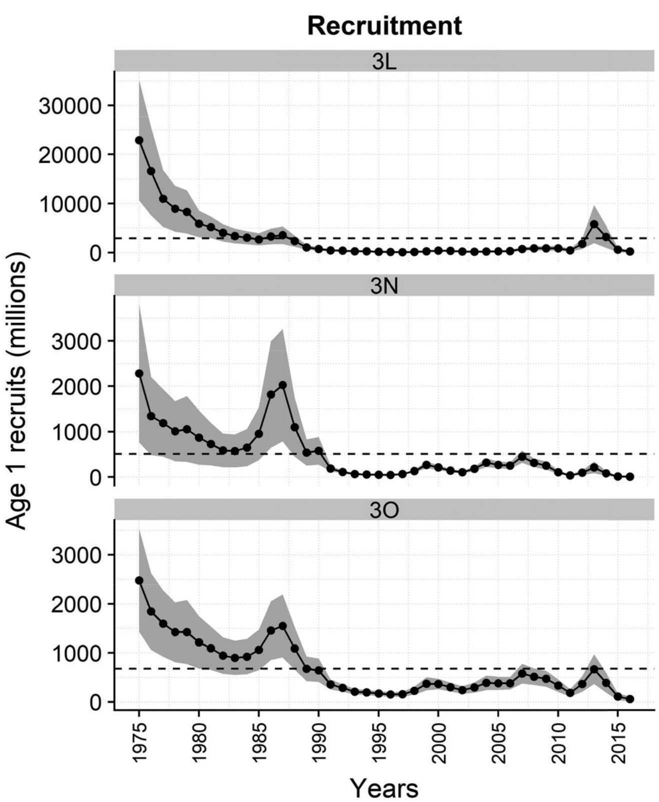

smaller mesh size than the previously used Engels trawl, but this does not necessarily represent an increase in age 1 fish in the ecosystem.

Fishing mortality rate (F)

The trends of estimated *F* values in divisions 3N and 3O are similar (Fig. 7), and this is substantiated by the high estimate of correlation coefficient for the spatially correlated year effects (Fig. A7). *F* is estimated to be the highest around the mid-1990s, with *F* peaking in 3L prior to that in 3N and 3O (Fig. 7). The peaks follow precipitous declines in all the divisions in the late 1990s. After the moratorium, *F* declined for about 5 years. This was followed by a short period of high mortality between the early to mid-2000s. The model also produces an increase in *F* in recent years. There is a peak in *F* in 2014, especially for 3L. This is possibly an outcome of an anomalous year for bycatch, or the parameter *F* is confounding with other mortality events (i.e., *M*) in the population. We have implemented stochasticity in *F*, but because we do not include catch data in fitting, it is not possible to separate process error or additional variability in *M* from *F*. Any events that bring process error to the state equation are absorbed by the stochasticity parameterizations for *F*. The estimates for all the six mean *F* are presented in Table A1.

The estimated landings trends for each division are computed using Baranov's catch equation, which are summed to provide estimates of annual total landings. These are only trends in landings because SSURBA only provides relative estimates of stock size. The landings data are not used to fit the SSURBA model, but we partially validate the estimated *F* values by providing a comparison of the reported and SSURBA estimated landings trends for each division and the whole stock (3LNO combined). The general trends are mostly similar; however, there are some differences, particularly in 3N and 3O, where the observed trends are considerably higher in the period from 1985 to 1990 in 3N and from 1985 to 1994 in 3O. There are also some discrepancies in the recent years, where predicted trends are slightly higher than the observed in all divisions (Fig. 10).

Survey gear catchability

The parameters *L*50 and *L*95 (eq. 14) for the Engel trawl catchability are estimated around 30.2 and 39.1 cm, respectively. As expected, the estimates of *L*50 and *L*95 for the Canadian and EU–Spanish Campelen trawls are smaller than those for the Engel trawl — *L*50 estimates are 17.8 and 21.7 cm and *L*95 estimates are 26.0 and 29.7 cm, respectively (Fig. 11). The estimates for the *q* scaling parameter Ω for the EU–Spanish gear is about 1.08. We are uncertain about the nearly 4 cm difference in both the parameters between Canadian and EU–Spanish versions of Campelen indices, considering that both the gears have similar construction except for the difference in the length of sweep lines. The EU–Spanish surveys cover deeper areas along the edge of the Grand Banks, and the differences in parameter estimates could originate from differences related to habitat and fish distribution or small differences in gear and sampling strategies. As mentioned before, the spatiotemporal changes in fish length make catchability-at-age dynamic; it changes with year, division, survey time (fall and

Fig. 10. Comparison of trend in predicted landings against the reported (observed) landings. The panels show Divisions 3L, 3N, 3O and the combined total for 3LNO.

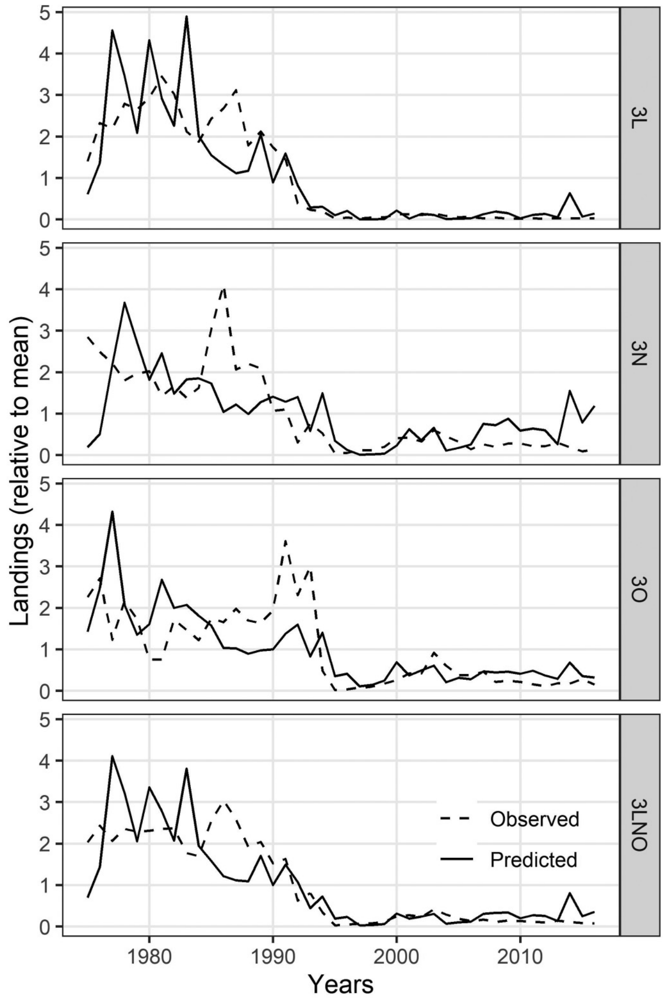

spring), and survey gears (Figs. A8 and A9). Owing to the smaller mesh size of the Campelen trawl compared with the Engel trawl, there is a sharp increase in the catchability-at-age in all the divisions, especially at younger ages, after the introduction of Campelen trawl in Canadian RV survey in the mid-1990s (Fig. A8). We also note a small increase in catchability for age 1 and age 2 in 2013–2016, especially for the spring survey, and this is due to a small increase in mean length-at-age of the fish of these age groups.

Stock performance

Relative B and SSB

Biomass trends show a rapid decline between the late 1970s and mid-1990s across all the divisions (Fig. 12). SSB follows almost similar trends as biomass. Biomass and SSB have remained at low levels in Divisions 3LO, with a little sign of improvement in 3N in the last decade; however, in the last 2 years, biomass and SSB estimates declined in 3N (Fig. 12). The SSURBA allows for comparisons of temporal changes in relative contributions of the three divisions in the total stock biomass and SSB (Fig. A10). Before the mid-1990s, 3L contributed a major proportion of the stock biomass and SSB, but after that 3N gradually surpassed 3L and by early 2000s became the major contributor to the stock biomass and SSB.

Fig. 11. Estimated logistic catchability of survey trawls: Engel, Canadian, and Spanish Campelen.

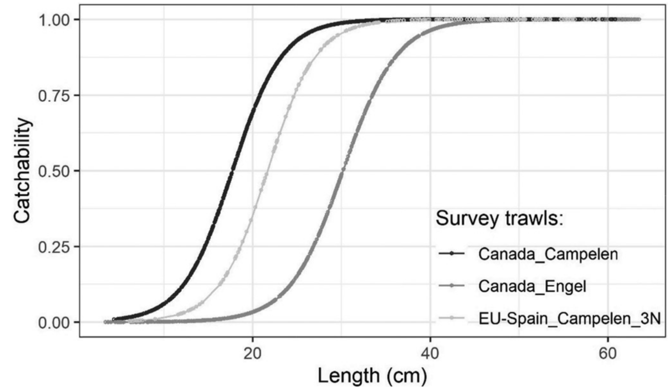

Landings or catch (C)

Historically, combined landings in 3LNO peaked in the 1980s, and the bulk of the catch came from 3L. A sharp decline in both the reported and the predicted series occurred in the late 1980s and early 1990s. The catch reached historically low levels by the mid-1990s, when a moratorium on directed fishing was imposed. Postmoratorium, the predicted landings for bycatch continues to be at low levels with some fluctuations without showing any strong trends, except in 3N where the SSURBA predictions are noticeably higher in recent years. (Fig. 10).

Discussion

Previous applications of SURBA models found that selectivity, catchability, and mortality were generally confounded and struggled to find a model fit without making assumptions about one of these factors (Cook 2013). Usually, survey catchability is fixed when fitting SURBA. To address the confounding, we combine the parameterization of survey selectivity and catchability into a parametric model for length-based catchability. The differences in fish length between the spring and fall, together with the assumption that length-based catchability parameters for the Canadian spring and fall surveys are the same, help us estimate the survey catchability pattern in age for all the gears. However, like SURBA, our SSURBA model assumes that the fully selected q for the spring and fall surveys is 1. Natural mortality is size-dependent and modelled as a function of fish weights (Lorenzen 1996; Miller and Hyun 2017). The underlying auxiliary cohort-based model for length-at-age used for implementing size-based catchability and natural mortality allows q and M to vary with temporal and spatial changes in fish growth and with change in population age structure. Through this approach we have tried to incorporate the effects of plasticity in growth on q and M and reduce biases in the stock assessment model stemming from assumptions of invariance (Lorenzen 2016). The length-based approach also inherently adjusts the catchability for length-at-age of cohorts at the time of the survey allowing a better fit to spring and fall survey data. This treatment of q and M reduces confounding of key parameters. As with other survey-based models, estimations of biomass and SSB using this model are relative to the assumption of catchability. The assumption of size-dependent M contributes to determining the scale of the model. It is relatively common to assume that $q = 1$ in trawl sampling (Walsh 1997), although factors like trawl swept area, light intensity, depth of tow, and density of fish could change survey catchability for a species. Such changes are difficult to estimate with SSURBA.

In comparison with ADAPT, the SSURBA predicts slightly higher abundance, biomass, and SSB since about 2005 (Fig. 13) — this is likely because of the several differences between SSURBA and ADAPT. For example, the SSURBA model fits to indices from dif-

Fig. 12. Temporal changes in biomass and spawning stock biomass (SSB) in the three Divisions 3LNO. Shades represent the 95% confidence interval around the estimates.

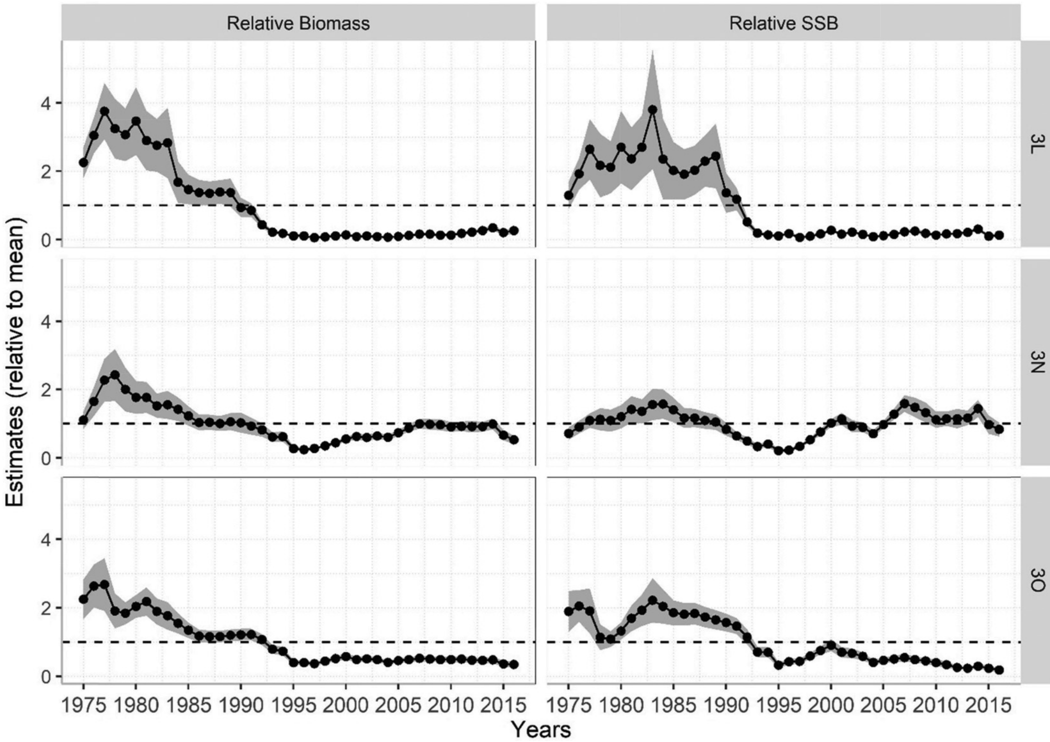

Fig. 13. Comparisons of our SSURBA model outputs for stock abundance, biomass, and spawning stock biomass (SSB) with the corresponding outputs from VPA-ADAPT model, which is currently used for the assessment of this stock.

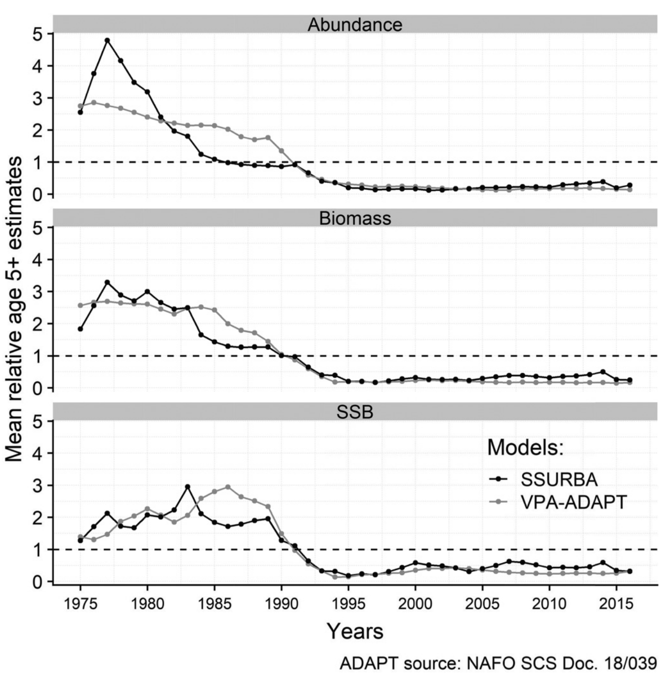

Fig. 14. A comparative presentation of average F for ages 9 to 14 estimated from the two models: SSURBA and VPA-ADAPT. Note that the average is weighted on corresponding abundance-at-age.

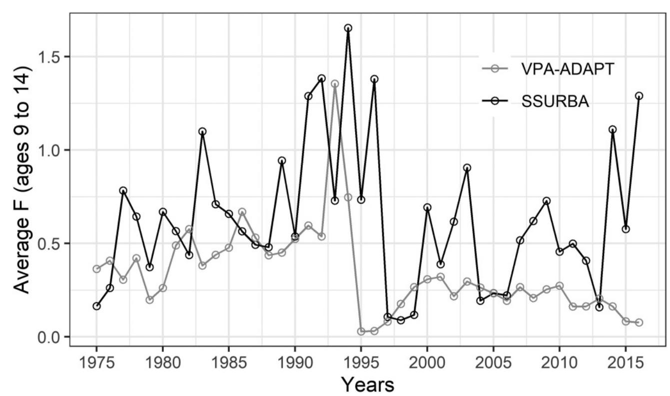

ferent divisions separately. Further, M is modelled differently in ADAPT and SSURBA; ADAPT has assumed M separate for two time periods ($M = 0.53$ from 1989 to 1996; otherwise 0.2) and SSURBA, as outlined above, has time-varying M dependent on fish size. ADAPT provides a combined estimate for the stock area, while SSURBA allows comparison of trends between divisions; the contribution to total biomass and SSB is highest from division 3N for the last couple of decades (Fig. A10). Though total catch or catch-at-age records are not part of the fitting process, total landings predictions from SSURBA have similar trends with the reported landings; however, there are periods from 1985 to 1990 where SSURBA is not able to predict the higher reported landings in 3LNO combined (Fig. 10). SSURBA predictions also differ from the reported landings in the recent years — the predictions are larger since 2014, and this is mainly noticeable in 3N. This difference is more prominent in the comparison of F estimates from ADAPT and SSURBA (Fig. 14). While SSURBA does not incorporate catch, ADAPT assumes that catches are known exactly, an assumption that is unlikely to hold particularly when all removals are bycatch. On the contrary, as we have explained previously, model stochasticity is included in F parameterization; hence, it is also possible that high predictions of *F* from SSURBA actually represent unexplained causes that have resulted in fish mortality.

When a stock covers a large area, it is quite possible that we observe geographic variation in phenotypic and population processes within the spatial distribution of the stock (Maunder et al. 2018). Many authors have used "areas as fleets" approaches using spatially structured fleets to parameterize the geographic variation (Punt et al. 2016), but this approach is suitable when the fishery is a leading driver for the spatial heterogeneity, or the fisheries selectivity–mortality can be utilized to account for spatial differences. We have adopted a more direct approach to define a spatial model to account for spatial differences in fish growth, to speculate about differences in productivity, and to explore spatial management options. Prior to developing this spatial SURBA model, we used the research survey data to compare correlation in recruitment trends among NAFO Divisions 2J3KLMNOPs. This analysis showed that there was high correlation in recruitment among the Grand Banks Divisions 3LNO (Kumar et al. 2019), which agrees with the results here. SSURBA modelling approach provides some suggestions for spatial management. Recruitment has been below average in all divisions in the last decade, except for an increase in 2013–2014 in 3L (Fig. 9). The SSURBA model also estimates high correlations and is also able to point towards difference in current productivity levels among the divisions, as shown in Fig. A11. In all the divisions, there has been a decline in productivity leading up to the moratorium. In 3N, the model predicts that the current SSB is similar to the that in the 1990s, but the productivity has declined. In 3L and 3O, SSB continues to be low postmoratorium, but productivity levels are maintained. It shows that current stock status in 3N is better than that in 3L and 3O, but productivity is lower.

Our model misses one key component of spatial models, which is movement between spatial areas. Larval modelling done for shrimp (*Pandalus borealis*) has suggested movement from north to south following the Labrador Current (Le Corre et al. 2019), so it is likely that American plaice SSB in 3L supports some recruitment in 3N and 3O, but not vice-versa unless mature fish from 3N and 3O move into 3L for spawning. Also, postsettlement tagging experiments have suggested that there is limited movement in American plaice (COSEWIC 2009); therefore, we need a better understanding of movement before we can make conclusive recommendations for spatial fishery management.

Overall, we extend the survey-based modelling framework to explore spatial management questions. Stock status and fishing mortality trends are produced for the three divisions, although making catch recommendations is not possible. The Canadian RV survey focusses on multiple species; therefore, the methodology presented here can be applied to several species, especially for stocks with limited fisheries catch information.

Acknowledgements

Research funding to RK was provided by the Ocean Choice International Industry Research Chair program at the Marine Institute of Memorial University of Newfoundland. Research funding to NC was provided by the Ocean Frontier Institute, through an award from the Canada First Research Excellence Fund. We thank Laura Wheeland and Bob Rogers from Fisheries and Oceans Canada, as well as Diana González-Troncoso and Irene Garrido from Instituto Español de Oceanografía, for providing us the data required for the modelling exercise. We also thank the many people involved in the collection and processing of these data.

References

Beare, D., Needle, C., Burns, F., and Reid, D. 2005. Using survey data independently from commercial data in stock assessment: an example using haddock in ICES Division VIa. ICES J. Mar. Sci. **62**(5): 996–1005. doi:10.1016/j.icesjms.2005.03.003.

Busby, C., Morgan, M., Dwyer, K., Fowler, G., Morin, R., Treble, M., et al. 2007. Review of the structure, the abundance and distribution of American plaice (*Hippoglossoides platessoides*) in Atlantic Canada in a species-at-risk context. DFO Canadian Science Advisory Secretariat. Sci. Advis. Rep. (2007/069).

Butterworth, D.S., and Rademeyer, R.A. 2008. Statistical catch-at-age analysis vs. ADAPT-VPA: the case of Gulf of Maine cod. ICES J. Mar. Sci. **65**(9): 1717–1732. doi:10.1093/icesjms/fsn178.

Cadigan, N. 2010. Trends in Northwest Atlantic Fisheries Organization (NAFO) Subdivision 3Ps Cod (*Gadus morhua*) stock size based on a separable total mortality model and the Fisheries and Oceans Canada Research Vessel survey index. Canadian Science Advisory Secretariat, Fisheries and Oceans Canada (Research Document 2010/05).

Cook, R. 1997. Stock trends in six North Sea stocks as revealed by an analysis of research vessel surveys. ICES J. Mar. Sci. **54**(5): 924–933. doi:10.1006/jmsc.1997.0235.

Cook, R. 2013. A fish stock assessment model using survey data when estimates of catch are unreliable. Fish. Res. **143**: 1–11. doi:10.1016/j.fishres.2013.01.003.

COSEWIC. 2009. COSEWIC assessment and status report on the American plaice *Hippoglossoides platessoides*, maritime population, Newfoundland and Labrador population and Arctic population, in Canada. Committee on the Status of Endangered Wildlife in Canada, Ottawa.

de Valpine, P. 2002. Review of methods for fitting time-series models with process and observation error and likelihood calculations for nonlinear, non-Gaussian state-space models. Bull. Mar. Sci. **70**(2): 455–471.

DFO. 2011. Recovery potential assessment of American Plaice (*Hippoglossoides platessoides*) in Newfoundland and Labrador. DFO Can. Sci. Advis. Sec. Sci. Advis. Rep. (2011/030).

DFO. 2013. Stock Assessment of Northern (2J3KL) Cod in 2013. DFO Can. Sci. Advis. Sec. Sci. Advis. Rep. (2013/014).

DFO. 2019. Stock Assessment of NAFO Subdivision 3Ps Cod. DFO Can. Sci. Advis. Sec. Sci. Advis. Rep. (2019/009).

Doubleday, W.G. 1981. Manual on groundfish surveys in the Northwest Atlantic. NAFO Scientific Council Studies, **2**: p. 55.

Gavaris, S. 1988. An adaptive framework for the estimation of population size. Res. Doc. Can. Atl. Fish. Scient. Adv. Comm. 88/29. pp. 1–12.

Halliday, R., and Fanning, L. 2006. A history of marine fisheries science in Atlantic Canada and its role in the management of fisheries. Proc. N. S. Inst. Sci. **43**(2): 159–183. doi:10.15273/pnsis.v43i2.3641.

Harley, S.J., Myers, R.A., and Dunn, A. 2001. Is catch-per-unit-effort proportional to abundance? Can. J. Fish. Aquat. Sci. **58**(9): 1760–1772. doi:10.1139/f01-112.

Hewitt, D.A., and Hoenig, J.M. 2005. Comparison of two approaches for estimating natural mortality based on longevity. Fish. Bull. **103**(2): 433.

Hoenig, J.M. 1983. Empirical use of longevity data to estimate mortality rates. Fish. Bull. **82**(1): 898–903.

Kristensen, K., Nielsen, A., Berg, C.W., Skaug, H., and Bell, B. 2016. TMB: automatic differentiation and Laplace approximation. J. Stat. Softw. **70**(5): 1–21. doi:10.18637/jss.v070.i05.

Kumar, R., Cadigan, N.G., and Morgan, M.J. 2019. Recruitment synchrony in spatially structured Newfoundland and Labrador populations of American plaice (*Hippoglossoides platessoides*). Fish. Res. **211**: 91–99. doi:10.1016/j.fishres.2018.10.027.

Le Corre, N., Pepin, P., Han, G., Ma, Z., and Snelgrove, P.V. 2019. Assessing connectivity patterns among management units of the Newfoundland and Labrador shrimp population. Fish. Oceanogr. **28**(2): 183–202. doi:10.1111/fog.12401.

Legault, C.M. 2011. Survey design efficiency of DFO and NEFSC surveys for cod, haddock, and yellowtail flounder on Georges Bank. Fisheries and Oceans Canada (2011/06).

Lorenzen, K. 1996. The relationship between body weight and natural mortality in juvenile and adult fish: a comparison of natural ecosystems and aquaculture. J. Fish Biol. **49**(4): 627–642. doi:10.1111/j.1095-8649.1996.tb00060.x.

Lorenzen, K. 2016. Toward a new paradigm for growth modeling in fisheries stock assessments: embracing plasticity and its consequences. Fish. Res. **180**: 4–22. doi:10.1016/j.fishres.2016.01.006.

Mangel, M. 2006. The theoretical biologist's toolbox: quantitative methods for ecology and evolutionary biology. Cambridge University Press.

Maunder, M.N., and Piner, K.R. 2014. Contemporary fisheries stock assessment: many issues still remain. ICES J. Mar. Sci. **72**(1): 7–18. doi:10.1093/icesjms/fsu015.

Maunder, M.N., Sibert, J.R., Fonteneau, A., Hampton, J., Kleiber, P., and Harley, S.J. 2006. Interpreting catch per unit effort data to assess the status of individual stocks and communities. ICES J. Mar. Sci. **63**(8): 1373–1385. doi:10.1016/j.icesjms.2006.05.008.

Maunder, M.N., Thorson, J.T., and Xu, H. 2018. Using spatio-temporal models of tagging data to deal with incomplete mixing. *In* Spatial stock assessment models workshop at Center for the Advancement of Population Assessment Methodology (CAPAM), Fisheries Science Center, La Jolla, CA, U.S.A., 1–5 October 2018 [online]. Available from http://capamresearch.org/sites/default/files/Maunder%20Mixing.pdf.

Mayo, R.K. 2003. Appendix 2: Woods Hole version of ADAPT/VPA Fisheries Assessment Compilation Tool Box (FACT). (36). NAFO Sci. Coun. Studies. pp. 163–199.

McCallum, B.R., and Walsh, S.J. 1996. Scientific Concil meeting-June 1996: Groundfish survey trawls used at the Northwest Atlantic Fisheries Centre, 1971–present. Northwest Atlantic Fisheries Organization (NAFO SCR Doc. 96/50).

Methot, R.D., Jr., and Wetzel, C.R. 2013. Stock synthesis: a biological and statistical framework for fish stock assessment and fishery management. Fish. Res. **142**: 86–99. doi:10.1016/j.fishres.2012.10.012.

Miller, T.J., and Hyun, S.-Y. 2017. Evaluating evidence for alternative natural mortality and process error assumptions using a state-space, age-structured assessment model. Can. J. Fish. Aquat. Sci. **75**(5): 691–703. doi:10.1139/cjfas-2017-0035.

Morgan, M. 1996. Preliminary results of tagging experiments on American plaice in NAFO Divisions 3LNO. Northwest Atlantic Fisheries Organization (NAFO SCR Doc. 96/61).

Morgan, M.J., Brodie, W., Bowering, W., Parsons, D.M., and Orr, D. 1998. Scientific Concil meeting-June 1998: Results of data conversions for American plaice in Div. 3LNO from comparative fishing trials between the Engel Otter trawl and the Campelen 1800 shrimp trawl. Northwest Atlantic Fisheries Organization (NAFO SCR Doc. 98/70).

Needle, C. 2002. Preliminary analyses of survey indices for whiting in IV and VIId. Working Document WD2 to the ICES Working Group on the Assessment of Demersal Stocks in the North Sea and Skagerrak, Copenhagen.

Newman, K., Buckland, S.T., Morgan, B., King, R., Borchers, D.L., Cole, D., et al. 2014. Modelling population dynamics. Springer, New York.

Nielsen, A., and Berg, C.W. 2014. Estimation of time-varying selectivity in stock assessments using state-space models. Fish. Res. **158**: 96–101. doi:10.1016/j.fishres.2014.01.014.

Pennino, M.G., Conesa, D., López-Quílez, A., Munoz, F., Fernández, A., and Bellido, J.M. 2016. Fishery-dependent and-independent data lead to consistent estimations of essential habitats. ICES J. Mar. Sci. **73**(9): 2302–2310. doi:10.1093/icesjms/fsw062.

Perreault, A.M., Zheng, N., and Cadigan, N.G. 2019. Estimation of growth parameters based on length-stratified age samples. Can. J. Fish. Aquat. Sci. **77**(3): 439–450. doi:10.1139/cjfas-2019-0129.

Peterson, I., and Wroblewski, J. 1984. Mortality rate of fishes in the pelagic ecosystem. Can. J. Fish. Aquat. Sci. **41**(7): 1117–1120. doi:10.1139/f84-131.

Petitgas, P., Cotter, J., Trenkel, V., and Mesnil, B. 2009. Fish stock assessments using surveys and indicators. Aquat. Living Resour. **22**: 119. doi:10.1051/alr/2009014.

Power, D., Healey, B., and Ings, D. 2015. Scientific council meeting – June 2015: Performance and description of Canadian multi-species bottom trawl surveys in NAFO subarea 2 + Divisions 3KLMNO, with emphasis on 2012–2014. Northwest Atlantic Fisheries Organization (NAFO SCR Doc. 16/28).

Punt, A.E., Haddon, M., Little, L.R., and Tuck, G.N. 2016. The effect of marine closures on a feedback control management strategy used in a spatially aggregated stock assessment: a case study based on pink ling in Australia. Can. J. Fish. Aquat. Sci. **74**(11): 1960–1973. doi:10.1139/cjfas-2016-0017.

R Core Team. 2019. R: A language and environment for statistical computing. R Foundation for Statistical Computing, Vienna, Austria.

Rago, P.J. 2005. 12. Fishery independent sampling: survey techniques and data analyses. Management techniques for elasmobranch fisheries. F.F.T. Paper. FAO Fisheries Technical Paper, No. 474. Rome, FAO.

Schnute, J.T., Boers, N., Haigh, R., Couture-Beil, A., Chabot, D., Grandin, C., et al. 2019. Package 'PBSmapping'. Fisheries and Oceans Canada, Pacific Biological Station (PBS) in 'Nanaimo', British Columbia, Canada.

Smith, J.S. 1996. Analysis of data from bottom trawl surveys. NAFO Scientific Council Studies, **28**: 25–53.

Smith, M.S. 1970. Report of the trawling operations of the Canadian research vessel G. B. Reed off Vancouver Island British Columbia, September 9 to 25, 1970. Fisheries Research Board, Biological station, Nanaimo, BC (1117).

Smith, W.H., and Sandwell, D.T. 1997. Global sea floor topography from satellite altimetry and ship depth soundings. Science, **277**(5334): 1957–1962. doi:10.1126/science.277.5334.1956.

Thygesen, U.H., Albertsen, C.M., Berg, C.W., Kristensen, K., and Nielsen, A. 2017. Validation of ecological state space models using the Laplace approximation. Environ. Ecol. Stat. **24**(2): 317–339. doi:10.1007/s10651-017-0372-4.

TMB documentaion. 2019. The comprehensive TMB documentation: Multivariate distributions [online]. Available from https://kaskr.github.io/adcomp/_book/Densities.html [accessed September 2019].

Walsh, S.J. 1997. Efficiency of bottom sampling trawls in deriving survey abundance indices. NAFO Sci. Coun. Studies, **28**: 9–24.

Walsh, S.J., Paz, X., and Duran, P. 2001. Scientific Concil meeting-June 2001: A Preliminary investigation of the efficiency of Canadian and Spanish survey bottom trawls on the southern Grand Bank. Northwest Atlantic Fisheries Organization (NAFO SCR Doc. 01/74).

Warren, W., Brodie, W., Stansbury, D., Walsh, S., Morgan, M.J., and Orr, D. 1997. Scientific Concil meeting-June 1997: Analysis of the 1996 comparative fishing trial between the Alfred Needler with the Engel 145 trawl and the Wilfred Templeman with the Campelen 1800 trawl. Northwest Atlantic Fisheries Organization (NAFO SCR Doc. 97/68).

Wheeland, L., Dwyer, K., Morgan, M., Rideout, R., and Rogers, R. 2018. Scientifc council meeting — June 2018: An assessment of American plaice in Div. 3LNO. Northwest Atlantic Fisheries Organization (NAFO SCS Doc. 18/039).

Zheng, N., Cadigan, N., and Morgan, M.J. 2020. A spatiotemporal Richards–Schnute growth model and its estimation when data are collected through length-stratified sampling. Environmental and Ecological Statistics.

Appendix A

Appendix Figs. A1–A11 and Table A1 appear on the following pages.

Fig. A1. The estimates for age-wise, time-varying natural mortality rate for each division.

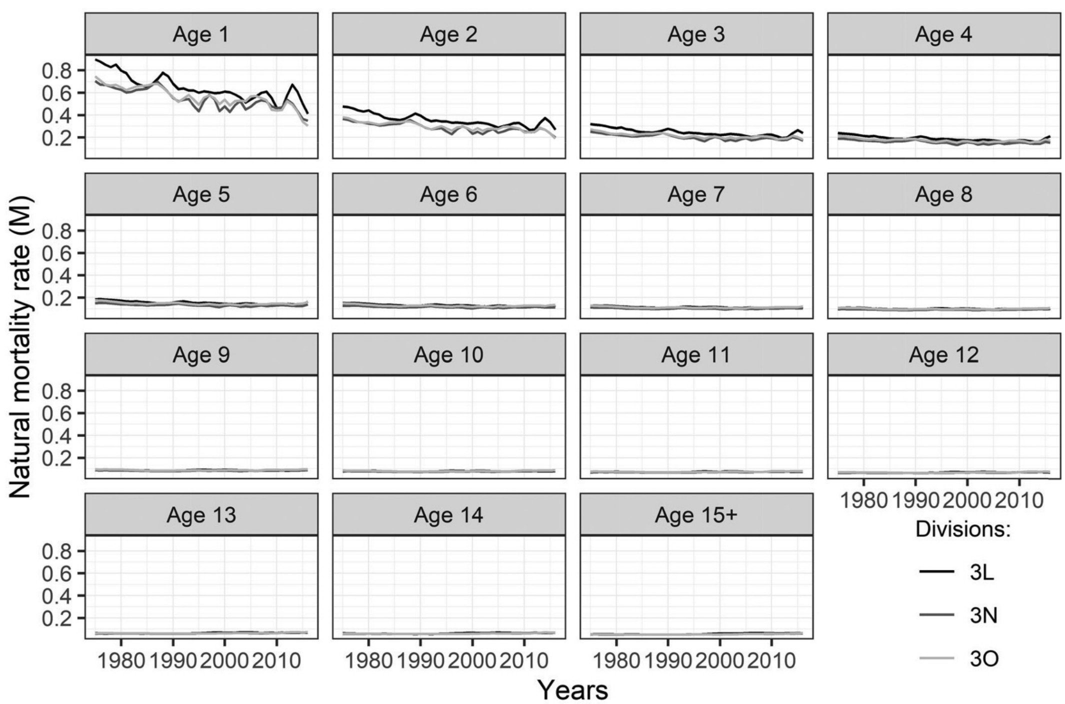

Fig. A2. Standardized residuals of indices obtained from the Canadian spring survey are plotted against year, cohort, age, and predicted log-index for the three divisions. A solid line representing the mean and a pair of dotted lines emphasizing ±2 marks on the *y* axis are drawn on each plot. Residuals for Engel indices are shown in blue. [Colour online.]

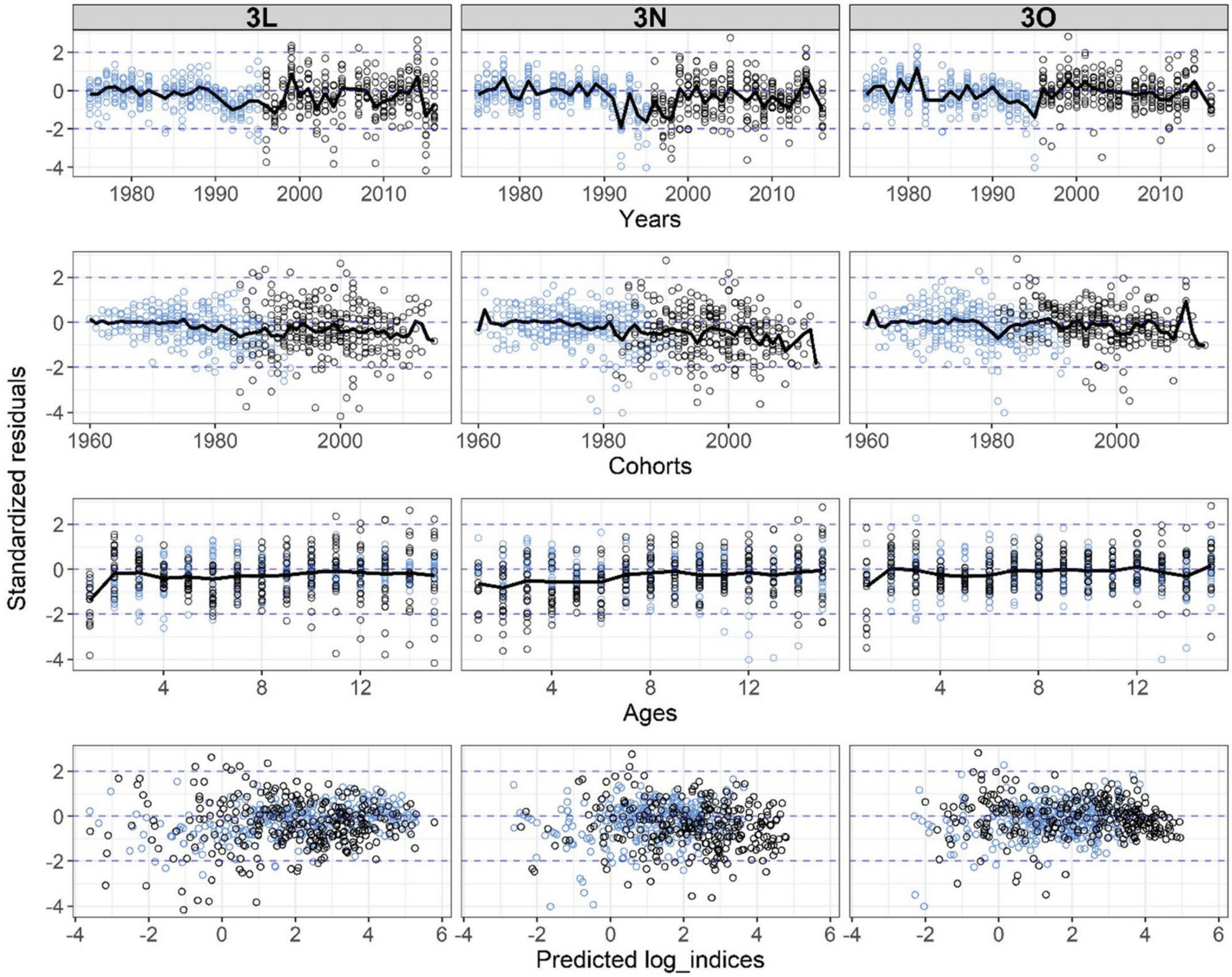

Fig. A3. Standardized residuals of indices obtained from the Canadian fall survey are plotted against year, cohort, age, and predicted log-index for the three divisions. A solid line representing the mean and a pair of dotted lines emphasizing ±2 marks on the *y* axis are drawn on each plot. Residuals for Engel indices are shown in blue. [Colour online.]

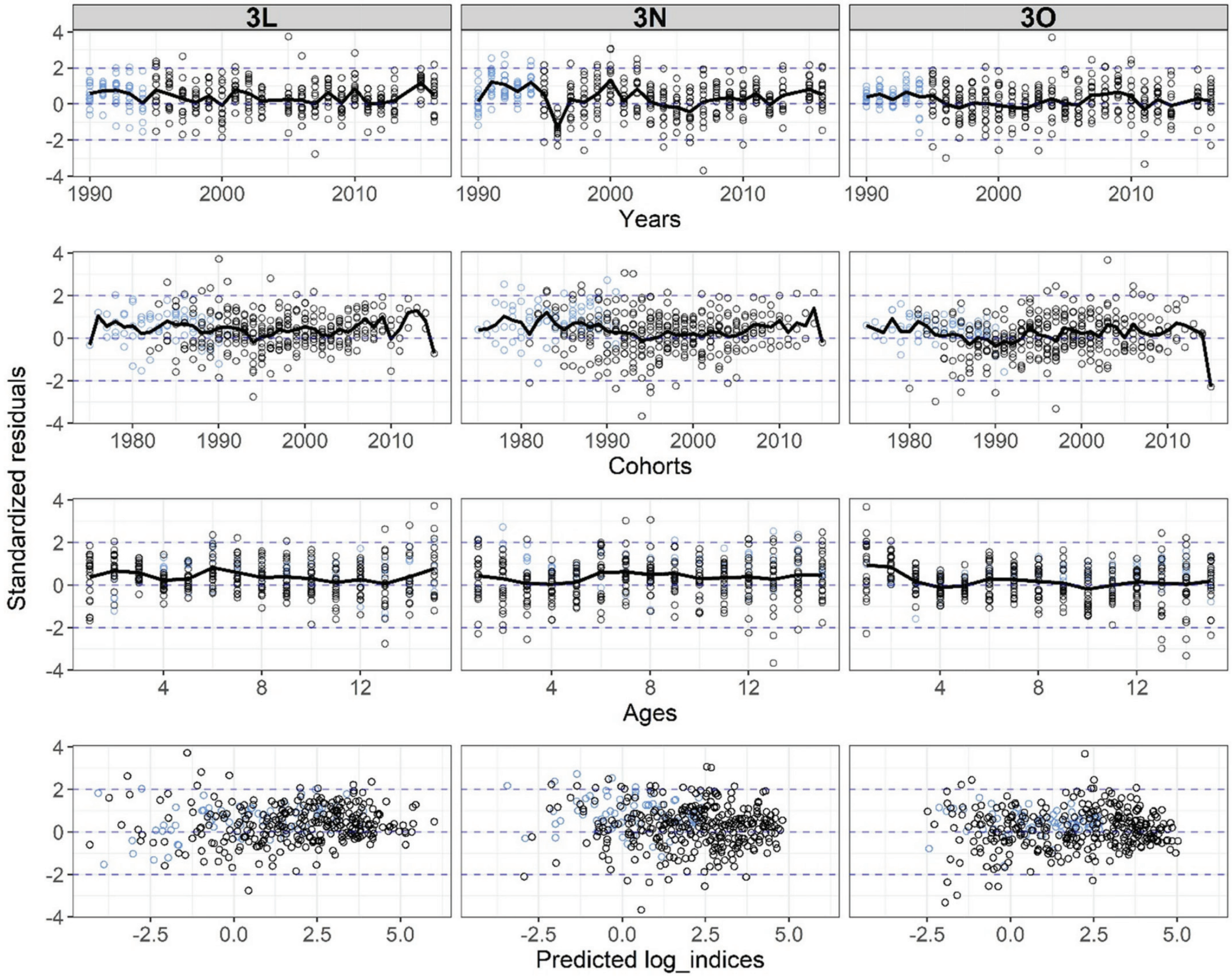

Fig. A4. Standardized residuals of indices obtained from the EU–Spanish survey are plotted against year, cohort, age, and predicted log-index for the three divisions. A solid line representing the mean and a pair of dotted lines emphasizing ±2 marks on the *y* axis are drawn on each plot.

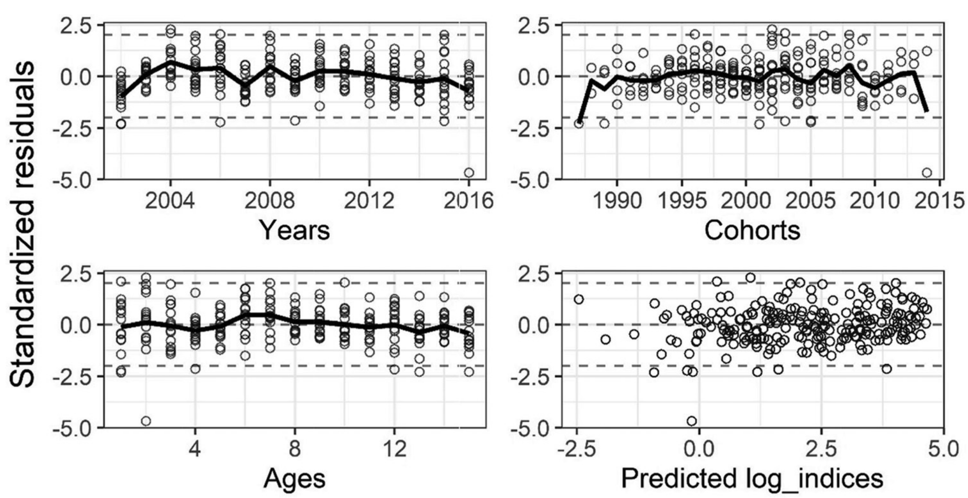

Fig. A5. A bar plot shows the estimates of abundance-at-age in the first year ($N_{a,1}$) in the Divisions 3LNO. Because of the large differences in the magnitude of $N_{a,1}$ among the divisions, for better clarity, we have added an inset figure zoomed at age 7 to age 15+ with its independent *y* axis.

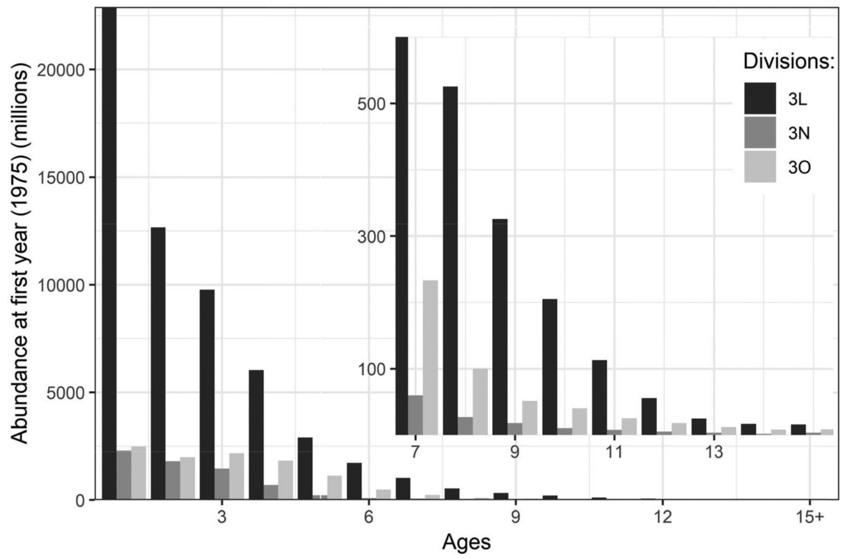

Fig. A6. A correlation matrix showing spatial correlation in the recruitment among the Divisions 3LNO.

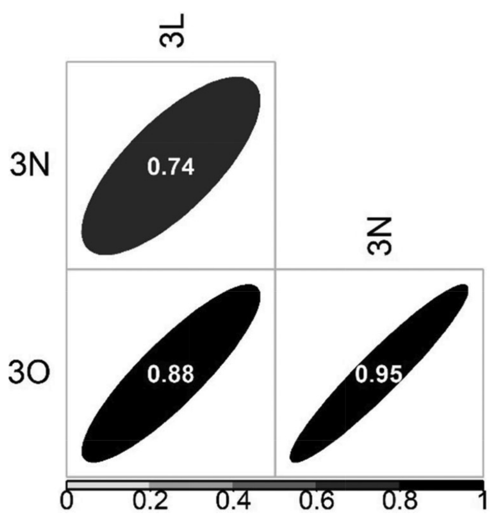

Fig. A7. Spatial correlation in *F* among the three Divisions 3LNO.

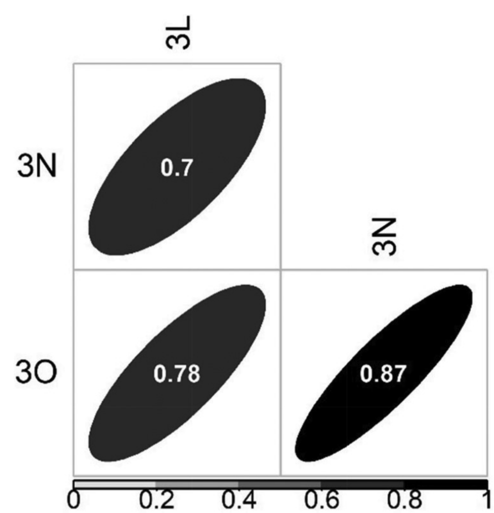

Fig. A8. Spatiotemporal changes in catchability-at-age for the Canadian trawl. Colours distinguish division, while dotted lines and solid lines represent spring and fall surveys, respectively. [Colour online.]

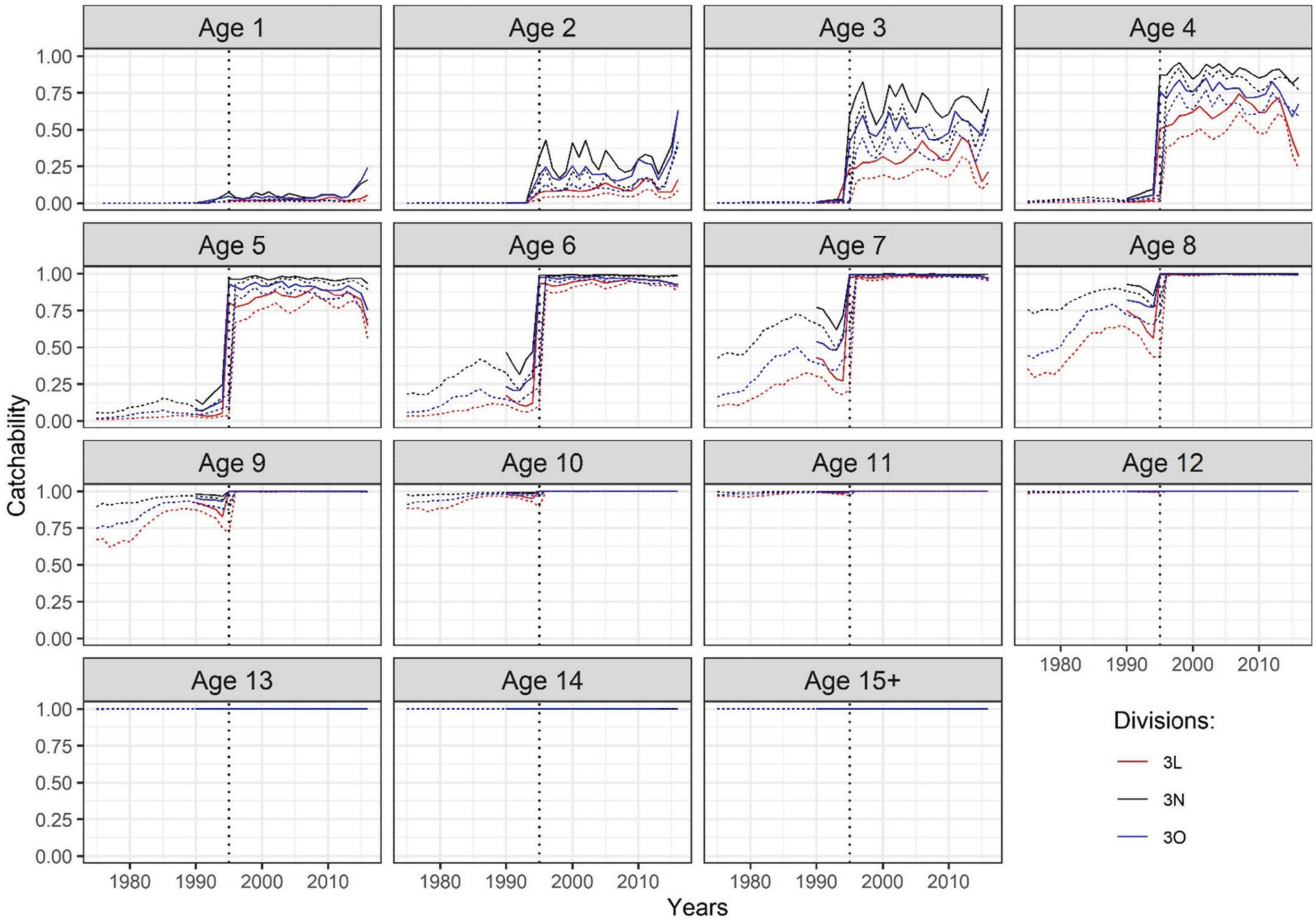

Fig. A9. Temporal changes in catchability-at-age for the Spanish trawl in NAFO Regulatory Area (NRA) of Division 3N.

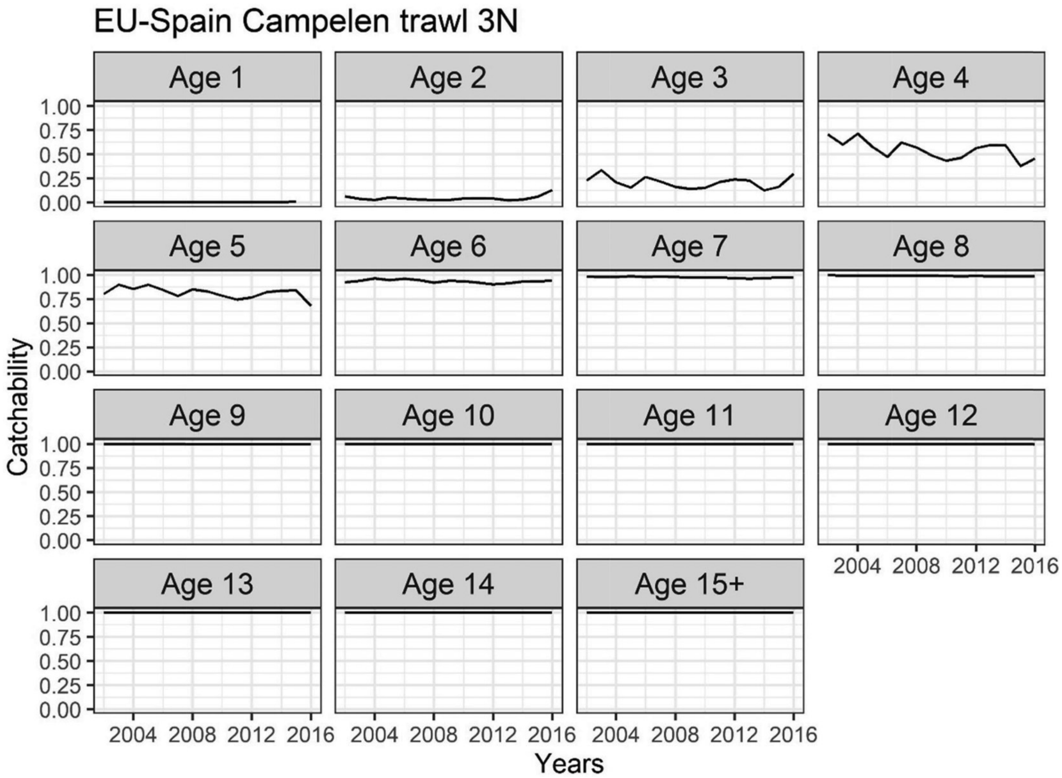

Fig. A10. Temporal changes in the relative contribution of the three divisions in the total stock recruitment, abundance, biomass, and spawning stock biomass (SSB).

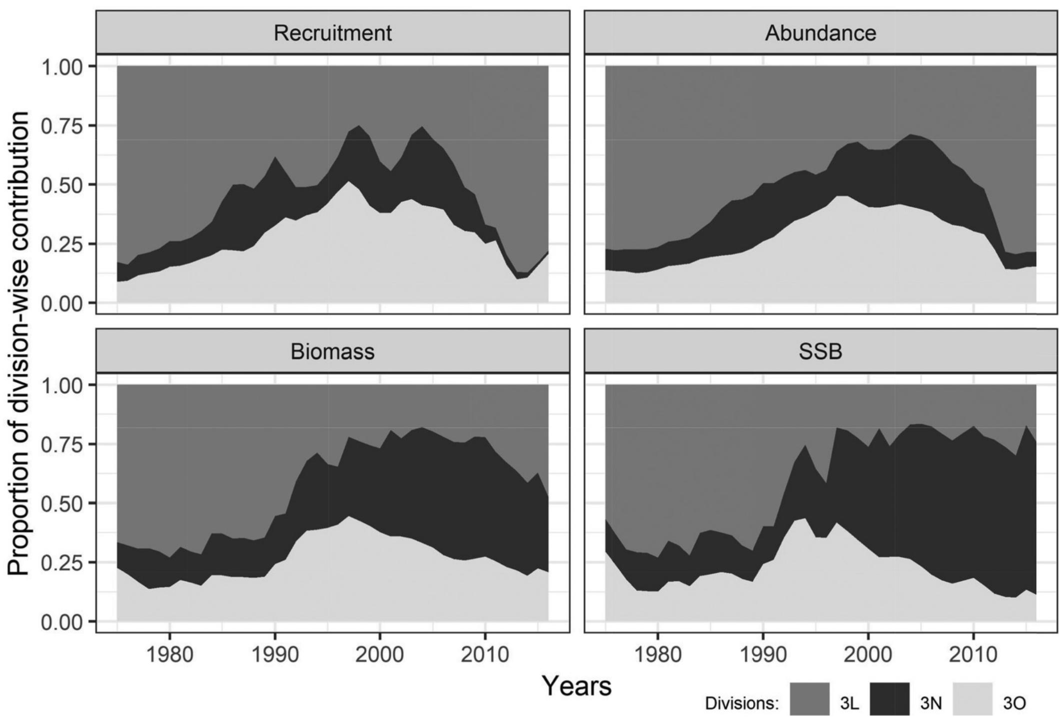

Fig. A11. Log of recruit-per-spawner (*R*/*S*) is plotted against log of spawning stock biomass (*SSB*) separately for the three Divisions 3LNO. To see the temporal variations in productivity, we connected points in chronological order of years.

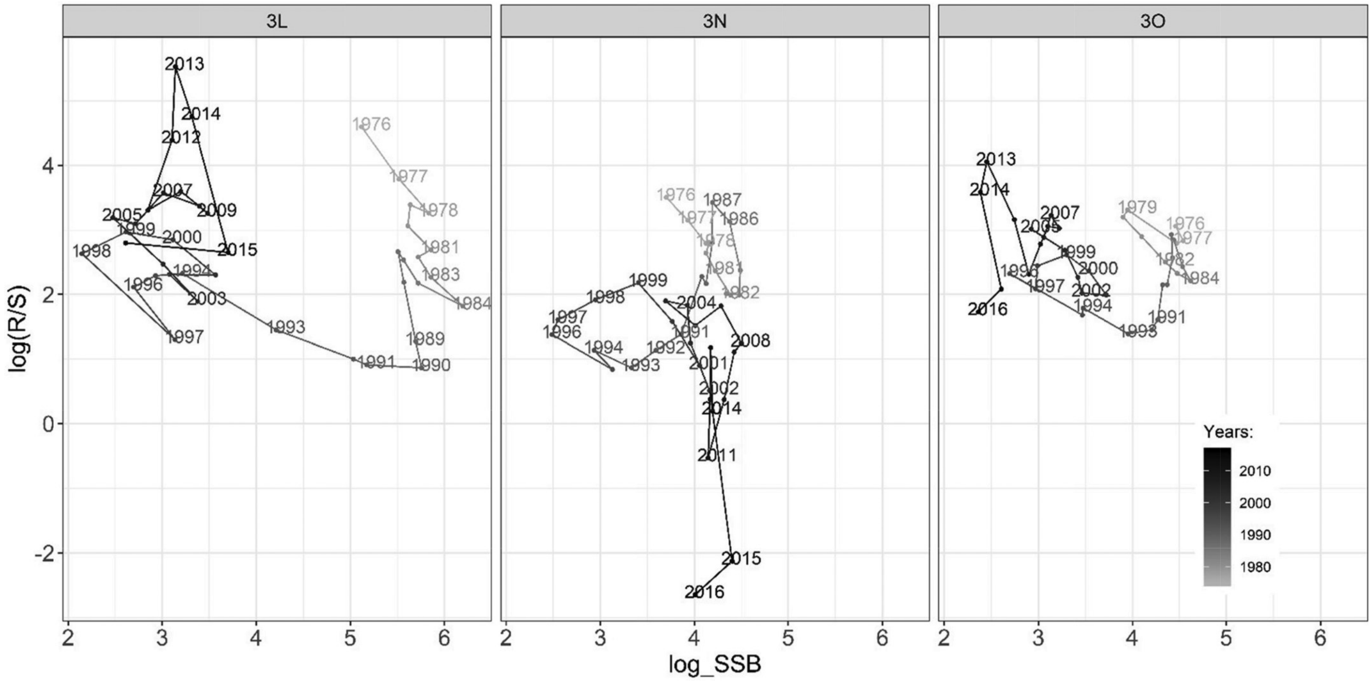

Table A1. All the mean *F* estimated in the model.

Division	Premoratorium	Postmoratorium
3L	0.45	0.22
3N	0.32	0.14
3O	0.63	0.30